INSTITUTO POTOSINO DE INVESTIGACIÓN CIENTÍFICA Y TECNOLÓGICA, A.C.

POSGRADO EN CIENCIAS AMBIENTALES

Production of Palladium nanoparticles in a microbial consortium for the reduction of 3,5,6-trichloro-2-pyridinol, metabolite of the insecticide Chlorpyrifos.

Tesis que presenta

Aries Berenice Figueroa Careaga

Para obtener el grado de

Maestra en Ciencias ambientales

Directora de la tesis:

Dra. Aura Ontiveros Valencia

San Luis Potosí, S.L.P. julio de 2023

Constancia de aprobación de la tesis

La tesis **"Production of Palladium nanoparticles in a microbial consortium for the reduction of 3,5,6-trichloro-2-pyridinol, metabolite of the insecticide Chlorpyrifos"** presentada para obtener el Grado de de Maestra en Ciencias Ambientales fue elaborada por **Aries Berenice Figueroa Careaga** y aprobada el **3 de julio de 2023** por los suscritos, designados por el Colegio de Profesores de la División de Ciencias Ambientales del Instituto Potosino de Investigación Científica y Tecnológica, A.C.

Dra. Aura Virginia Ontiveros Valencia
Directora de tesis

Dr. José René Rangel Mendez
Miembro del Comité Tutoral

Dr. Elias Razo Flores
Miembro del Comité Tutoral

Dr. Francisco Javier Cervantes Carrillo
Miembro del Comité Tutoral

Créditos Institucionales

This thesis was developed at the Environmental Sciences Division of Instituto Potosino de Investigación Científica y Tecnológica (IPICyT), A.C., under the supervision of Dr. Aura Virginia Ontiveros Valencia.

During the course of this work, the author received an academic scholarship from the National Council for Science and Technology (No**.** 1079846) and Instituto Potosino de Investigación Científica y Tecnológica (IPICyT), A.C.

Página en Blanco que se va a utilizar para colocar la copia del acta de examen

Dedicatoria

Esta tesis va dedicada a mi madre, Paty, y a mi hermana, Aranza, mi pequeña familia. Muchas gracias por hacerme sentir capaz de que puedo lograr todo lo que me proponga y por no dejarme renunciar ante la adversidad. Si las tengo a ustedes no hay obstáculo que no pueda vencer o meta que no pueda alcanzar. A su lado nunca me faltaron las risas ni las palabras de aliento, ustedes me inspiran a superarme cada día de mi vida. Gracias por todo su amor y por confiar en mí durante esta etapa. Espero encontrarlas siempre. Ustedes son mi cielo.

A mi padre, Javier, por alentarme a ser mejor en todo lo que me proponga, por sus valiosos consejos y por todo su amor y palabras de aliento a lo largo de mi vida. Gracias por estar presente pese a la distancia.

A mi abuela, Amelia, mi segunda madre. Todos los logros que he tenido y espero tener en un futuro van dedicados a ti. No sería la persona que soy ahora si no fuera por tus cuidados, tu paciencia, tu cariño y tu amor incondicional. Eres mi ejemplo a seguir y una de las razones principales por las que quiero ayudar al mundo. Estarás en mi corazón toda la vida.

A mi esposo, Antonio. No sé qué hubiera sido de mí durante esta etapa de mi vida sin tu apoyo. Siempre voy a agradecer tus viajes desde Ciudad de México hasta San Luis para verme, tus palabras de aliento, tu amor incondicional, tu paciencia al enseñarme a programar, tus bromas que endulzan mi vida y tus abrazos que me curan el alma.

Acknowledgements

First and foremost, I would like to express my heartfelt gratitude to Dr. Aura Ontiveros Valencia for the invaluable support extended to me throughout this journey. It was a tremendous honor to have been her first master's student, as well as the privilege of acquiring knowledge under her tutelage. Her guidance, both academically and in matters of life, has been marked by a remarkable display of patience and compassion. She has undoubtedly made this life-altering experience an indelible memory, characterized by profound joy, love, and utmost respect.

Special thanks to Dr. René Ragel Méndez for his expert professional guidance and invaluable support, as well as his helpful and constructive recommendations. I would also like to acknowledge his warm welcome into his research team.

I would like to thank to Dr. Elías Razo and Dr. Francisco Javier Cervantes for their useful critiques of this research work. Thank you for your advice and assistance.

I would also like to extend my gratitude to the technicians of the laboratory of the Environmental Sciences Division at IPICYT, M. Sc. Guillermo Vídriales Escobar and M. Sc Juan Pablo Rodas. Thaks to Q. Ma del Carmen Rocha Medina from Laboratorio Nacional de Biotecnología Agrícola, Médica y Ambiental (LANBAMA) and to Ana Iris Peña Maldonado from Laboratorio Nacional de Investigaciones en Nanociencias y nanotecnologías(LINAN)for their valuable technical support in this project.

I would like to thank the support of some wonderful people who provided me with their friendship during my stay in San Luis (some of them even before that). Their words of encouragement and advice helped me overcome academic and personal obstacles that once appeared insurmountable. So, thank you Enoé, Dendera, Paola, Cassandra, Paulina, Mónica, Chuy and Cristopper. Being able to regard you as friends fills me with immense happiness.

Last but not least, I wanna thank me, I wanna thank me for believing in me, I wanna thank me for doing all this hard work, I wanna thank me for having no days off, I wanna thank me for never quitting.

CONTENTS

Certificate of thesis approval ii
Institutional Support iii
Certificate of exam iv
Dedication v
Acknowledgements vi
List of tables x
List of figures xi
Abbreviations xiii
Resumen xiv
Abstract xv

1. INTRODUCTION 1
1.1. Chlorpyrifos 1
1.1.2. Degradation, fate, and transport 2
1.2. TCP 4
2. STATE OF ART FOR CP AND TCP: REMOVAL ALTERNATIVES 5
2.1. Physicochemical treatments 5
2.2. Biological treatments 6
2.3. Catalysts 11
3. JUSTIFICATION 16
4. HYPOTHESIS 16
5. OBJECTIVES 16
5.1. General 16
5.2. Specifics 16
6. MATERIALS AND METHODS 17
6.1. Source of sludge 17
6.2. Batch Pd(II) reduction experiments 18
6.3. TCP reduction experiments 19

6.4. Analytical techniques 20
6.5. Scanning electron microscopy 21
6.6. DNA extraction and microbial community analyses 21
6.7. Statistical analysis 22
7. RESULTS AND DISCUSSION 22
7.1. NPs synthesis 22
7.2. TCP reduction 28
7.3. Microbial community structure and diversity 34
8. CONCLUSIONS AND PERSPECTIVES 39
9. REFERENCES 42

List of tables

Table 1.	Pesticide classification criteria based on acute oral and dermal toxicity in rats according to median lethal dose (DL_{50})	2
Table 2.	Metabolites of CP that are formed during degradation	3
Table 3.	Properties of CP and TCP	5
Table 4.	Strains used for the biodegradation of CP and TCP	7
Table 5.	Bacteria used to produce metallic NPs.	12
Table 6.	Physico-chemical properties of Pd.	13
Table 7.	Solids characterization values (g/L)	18
Table 8.	Microcosms setup for Pd(II) reduction experiments	19
Table 9.	Microcosms setup for TCP reduction experiments	20
Table 10.	Pd(II) reduction kinetic values of the biotic and abiotic microcosms supplemented with H_2 (NPs-BH, NPs-AH) and glucose (NPs-BG, NPs-AG) at 24 h of incubation.	25
Table 11.	TCP reduction kinetic values of the different microcosms supplemented with H2 and glucose after 24h of incubation.	33

List of figures

Figure 1	Degradation pathway of CP	4
Figure 2	Anoxic sludge collected from WWTP Agua Tratada del Potosí, S.A. of C.V.	17
Figure 3	Kinetic evolution of Pd(II) reduction in biotic and abiotic microcosm supplemented with H_2 (■, ●) and glucose (▲, ◆). Where NPs-BH=NPs-Biotic H_2, NPs-AH=NPs-Abiotic H_2, NPs-BG= NPs-Biotic Glucose, and NPs-AG= NPs-Abiotic Glucose.	23
Figure 4	Black precipitates in the microcosms NPs-AH and NPs-BH.	24
Figure 5	On the left, SEM images of Pd in the abiotic (A, B) and inoculated (C, D) microcosms supplemented with H_2 (A, C), and glucose (B, D). On the right, EDS analysis corresponding to the samples shown in the SEM images.	28
Figure 6	TCP reduction kinetics in the microcosms supplemented with H2 (A) and glucose (B). Where, coupled= microbial consortia + Pd catalyst, no catalyst= lack of Pd catalyst, abiotic= lack of microbial consortia.	29
Figure 7	Relative abundances of phylotypes at the genus level for all the inoculated microcosms. All phylotypes (less than <1% relative abundance) are grouped and shown in gray. Where NPs-BH=NPs-Biotic H2, NPs-BG= NPs-Biotic Glucose, and NPs-DC= NPs-Donor control; coupled= microbial consortia + Pd catalyst, no catalyst= lack of Pd catalyst, abiotic= lack of microbial consortia and TCP-DC= TCP without electron donor.	33
Figure 8	Alpha diversity indexes for all microcosms. Where NPs-BH=NPs-Biotic H2, NPs-BG= NPs-Biotic Glucose, and	37

NPs-DC= NPs-Donor control; coupled= microbial consortia + Pd catalyst., no catalyst= lack of Pd catalyst, abiotic= lack of microbial consortia and TCP-DC= TCP without electron donor.

Figure 9 Betha diversity indexes for all microcosms. Where NPs-BH=NPs-Biotic H2, NPs-BG= NPs-Biotic Glucose, and NPs-DC= NPs-Donor control; coupled= microbial consortia + Pd catalyst., no catalyst= lack of Pd catalyst, abiotic= lack of microbial consortia and TCP-DC= TCP without electron donor. 38

Abbreviations

CP	Chlorpyrifos
DETP	Diethylthiophosphate
H_2	Hydrogen
N_2	Nitrogen
OP	Organophosphate
TCP	3,5,6-trichloro-2-pyridinol

RESUMEN

El 3,5,6-tricloro-2-piridinol (TCP) es el metabolito más tóxico del insecticida organofosforado clorpirifos (CP), que genera una contaminación generalizada de suelos y cuerpos acuáticos, lo cual suscita preocupación por su dispersión en el medio ambiente y la necesidad de tratamiento. Una alternativa prometedora para reducir este contaminante es el uso de catalizadores a base de paladio (Pd), que pueden activar el hidrógeno (H_2) para promover la reducción de TCP.

En el presente estudio, se realizaron diversas configuraciones bióticas y abióticas de microcosmos utilizando H_2 y glucosa como donadores de electrones para promover la reducción microbiológica de Pd(II). Asimismo, se probaron siete tipos de configuraciones de microcosmos con H_2, glucosa y con o sin Pd(II) con sus respectivos controles como catalizadores para lograr la reducción de TCP.

Los resultados obtenidos en la producción de nanopartículas (NPs) de Pd indican que el microcosmo biótico que contenía Pd(II), y glucosa como donardor de electrones tuvo una reducción de Pd(II) mayor al 99% en un periodo de 24 horas de incubación. Es probable que este efecto se deba a la presencia de bacterias fermentativas que produjeron H_2 mediante la fermentación de glucosa que favoreció la producción de NPs de Pd. Al final del periodo de incubación, aparecieron materiales negros en el fondo de los microcosmos inoculados y no inoculados, lo que indicó la precipitación de Pd, lo cual fue posteriormente verificado por espectroscopía de rayos X.

Por otro lado, los resultados de la cinética de remoción de TCP mostraron que el microcosmo que contenía una comunidad microbiana y glucosa como donador, pero sin presencia de Pd, logró una remoción del 100% del contaminante en un periodo de 24 horas, con una tasa de reducción de 0.44 TCP/L-h. En contraste, el microcosmo biótico que contenía H_2 como donador, pero no catalizador, solo logró una reducción del 5.39 ±3.5% de TCP con una tasa de reducción de 0.02 mg TCP/L-h. Estos resultados sugieren que la presencia de TCP, conocido por sus propiedades antimicrobianas, pudo haber afectado la capacidad de los microorganismos para llevar a cabo la reducción del contaminante, particularmente cuando no se tenían las NPs de Pd como catalizador.

El análisis de la comunidad bacteriana de los microcosmos inoculados demostró que, independientemente de la presencia o ausencia de TCP, los filos Proteobacteria a nivel de género *Azospira* y *Thauera* estuvieron presentes con una abundancia relativa superior al 4%. El género *Clostridium*, encontrado en el microcosmo biótico con Pd(II), y glucosa como donador de electrones, representó el mayor porcentaje de bacterias reportadas (58.1%). No obstante, su abundancia relativa disminuyó en los experimentos de reducción de TCP debido a los efectos inhibitorios del contaminante.

Palabras clave: TCP, nanopartículas de paladio, catalizador, comunidades microbianas, contaminantes emergentes.

ABSTRACT

3,5,6-trichloro-2-pyridinol (TCP) is the most toxic metabolite of the organophosphate insecticide chlorpyrifos (CP), which generates widespread soil and aquatic pollution, raising concerns about its environmental dispersion and the need for treatment. A promising alternative to reduce this contaminant is the use of palladium (Pd)-based catalysts, which can activate hydrogen (H_2) to promote TCP reduction.

In this study, different biotic and abiotic microcosm configurations were used with H_2 and glucose as electron donors to promote microbial Pd(II) reduction. Additionally, seven types of microcosm configurations with H_2, glucose, and with or without Pd(II) with their respective controls were tested as catalysts to achieve TCP reduction.

The results of Pd nanoparticles production showed that the biological microcosm containing Pd(II) and glucose had a removal greater than 99% in reducing Pd(II) in a 24-hour incubation period. This effect is likely due to the presence of fermentative bacteria that produced H_2 through glucose fermentation, which favored Pd nanoparticles production. At the end of the incubation period, black materials appeared at the bottom of both inoculated and non-inoculated microcosms, indicating the precipitation of Pd, which was further verified by X-ray spectroscopy.

Besides, the results of TCP removal kinetics showed that the biological microcosm with glucose as an electron donor but no Pd, achieved 100% removal of the contaminant in a 24-hour period, with a reduction rate of 0.44 TCP/L-h. In contrast, the biological microcosm containing H_2 as a donor and microorganisms but no catalyst, only achieved a reduction of 5.39 ±3.5% of TCP with a reduction rate of 0.02 mg TCP/L-h. These results suggest that the presence of TCP, known for its antimicrobial properties, may have affected the ability of microorganisms to carry out TCP reduction specially when lacking the nanoparticles Pd catalyst.

Analysis of the bacterial community of all inoculated microcosm showed that regardless of the presence or absence of TCP, the Proteobacteria phyla for the *Azospira* and *Thauera* genus levels were present with a relative abundance greater than 4%. The *Clostridium* genus, found in the biological microcosm with Pd(II) and glucose as electron donor, represented the highest percentage of reported bacteria (58.1%). However, its relative abundance decreased in TCP reduction experiments due to the TCP inhibitory effects.

Key words: TCP, palladium nanoparticles, catalyst, microbial communities, emerging contaminant

1. INTRODUCTION

1.1. Chlorpyrifos

Pesticides have been employed on a global scale to enhance agricultural yields. Depending on the targeted pest, pesticides are classified by various names, such as herbicides, rodenticides, fungicides, and insecticides, among others. Specifically, insecticides are made of chemical or biological agents that are intended to manage insects by predominantly killing them through the inhibition of enzymes and interfere with the insect's nervous system. Organophosphates (OPs) are widely recognized as one of the most commonly utilized insecticides, as stated by the Environmental Protection Agency (EPA). They have been employed as alternatives to organochlorine and carbamate insecticides due to their remarkable efficacy, cost-effectiveness in production, and relatively lower toxicity levels[1–3].

Chlorpyrifos (CP) is a broad-spectrum moderately hazardous chlorinated OP insecticide (Table 1)[4,5]. It has been used since 1965 in various crops as a safer alternative to more hazardous OP compounds to control a wide range of pests such as cutworms, cockroaches, grubs, flea beetles, flies, termites, and lice[6–8]. CP is considered the fourth most used pesticide after endosulfan, acephate, and monocrotophos[9]. Its popularity ranked first on the list of the most commonly used OP insecticides in the US in 2007, 2009, and 2012. CP also ranked fourteenth in the top 25 most used conventional pesticide active ingredients in the agricultural sector in 2012[10].

Due to its effectiveness, affordability, and wide range of commercial uses, CP is utilized in economically significant crops. However, the excessive use of CP can result in its entry into the environment through spraying, runoff, and accidental spills. These activities have the potential to cause severe and enduring impacts on various aquatic and terrestrial species populations. Reports from around the world indicate the presence of CP in concentrations ranging from µg/L to mg/L in the air, water, and soil.[11–15].

Table 1. Pesticide classification criteria based on acute oral and dermal toxicity in rats according to median lethal dose (DL_{50})[5].

		DL_{50} for rats (mg/kg body weight)	
	Class	Oral	Dermal
Ia	Extremely hazardous	<5	<50
Ib	Highly hazardous	5-50	50-200
II	Moderately hazardous	50-2000	200-2000
III	Slightly hazardous	Over 2000	Over 2000
U	Unlikely to present acute hazard	5000 or higher	

This insecticide is a neurotoxic whose main mechanism of toxicity is expressed through the inhibition of the enzyme acetylcholinesterase. It can cause vomiting, lung and central nervous system damage, and developmental and autoimmune disorders[16,17]. However, the serious adverse effects of this insecticide are not only limited to humans, its toxicity to other mammals, fish, birds, and aquatic invertebrates have already been reported[6,11,18].

1.1.2. Degradation, fate, and transport

CP, similar to other OP pesticides, experiences various degradation pathways when present in the environment. During its degradation, primary and secondary metabolites are formed (Table 2). CP undergoes oxidation to its oxon form called CP-oxon. This CP-oxon can then be enzymatically or spontaneously hydrolyzed, resulting in the formation of Diethyl Phosphorothioate (DETP) and 3,5,6-trichloro-2-pyridinol (TCP) (illustrated in Figure 1). Additionally, TCP has the potential to undergo methylation, leading to the creation of 3,5,6-trichloro-2-methoxy pyridone, or it may undergo dechlorination.

Apart from the formation of CP-oxon, CP can also undergo oxidation mediated by cytochrome P-450 enzymes, forming an unstable intermediate that subsequently follows spontaneous hydrolysis, yielding DETP and TCP. When CP enters surface water, its degradation predominantly involves abiotic hydrolysis or photosensitized oxidation. In soil environments, photodegradation plays a significant role in

processes such as hydrolysis, dehalogenation, and oxidation of this particular insecticide.[15,16]

Respect to the degradation mediated by microorganisms, the microbial population located at the site of pesticide contamination can get adapted to CP high concentrations. Consequently, this adaptation can play an important role in the degradation process if the contaminant is not above the threshold level. Regarding CP's metabolism, it follows three pathways: alkylation, reductive dechlorination, and oxidative dechlorination pathway[19]. In the first pathway, the alkylation of CP generates TCP, which in turn generates secondary metabolites (Table 2).

In the reductive dechlorination pathway, the process of dechlorination completely decomposes CP until obtaining carbon dioxide, ammonia, water, and other inorganic materials. The oxidative dechlorination pathway of TCP has been demonstrated in microorganisms such as Bacillus subtilis and Micrococcus luteus, which can dechlorinate the ortho and para- Cl atoms of TCP through oxidation, resulting in the formation of 3,6-dihydroxypyridyl-2,5-diketone. This oxidative dechlorination is facilitated by the enzymes present in these microorganisms, which carry out biochemical and physiological reactions to break down and degrade the contaminant. This process is called enzymatic degradation.

Table 2. Metabolites of CP that are formed during degradation[7.]

Status of metabolite	Name of metabolite
Principal	CP-oxon
Primary	**TCP**
	DETP
Secondary	3,5,6-trichloro-2-metoxipyridone
	Clorodihydro-2-pyridone
	tetrahydro-2-pyridone
	Maleimide semialdehyde
	3,5,6-trichloro-2-metilpyridone
	3,6-dihydroxypyridil-2,5-dicetone

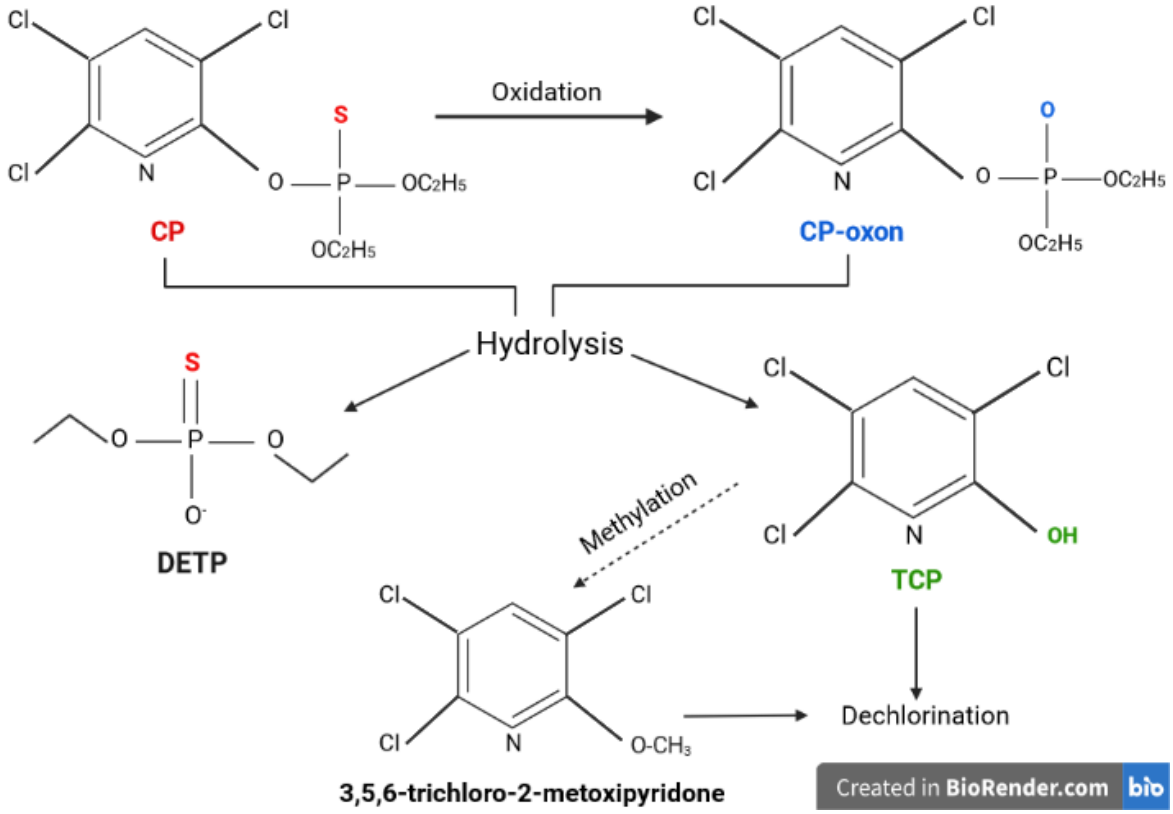

Figure 1. Degradation pathway of CP[15,20,21].

1.2. TCP

Among the metabolites of CP, TCP is even more toxic and persistent than CP, with a half-life from 65 to 365 days[22,23]. TCP has antimicrobial properties, which prevent the proliferation of microorganisms that could help with its degradation. In addition, TCP is more soluble in water than CP (Table 3), thus it is more leachable, causing great contamination in soils and aquatic environments[24].In fact, TCP has been detected in the blood[18] and urine of the general US population with concentrations in the range of µg/L[25]. Concentrations of this metabolite have also been found in the tissues of farm animals such as sheep, goats, and fish[22]. It should be noted that TCP excreted in the urine of humans and other mammals have frequently been used as an indicator of CP exposure[25].

Given the damage that CP and TCP can cause to humans and other organisms, several studies have tried to degrade these pollutants by using different treatments.

Table 3. Properties of CP and TCP[19,26]

Property	CP	TCP
Chemical name	O, O- diethyl 0-(3,5,6-trichloro-2-pyridinyl)-phosphorothioate	3,5,6- trichloro-2-pyridinol
Formula	$C_9H_{11}Cl_3NO_3PS$	$C_5H_2Cl_3NO$
Structure	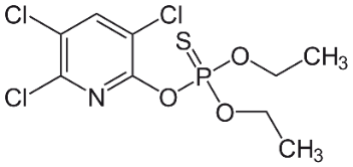	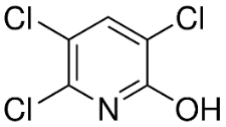
Molecular weight (g/mol)	350.62	198.43
Melting point (°C)	41-42	174-175
Solubility (mg/L) at 25°C	1.39	80.9
K_{oc} (ml/g)	9930	77-242
Half-life (días)	7-120	65-365

2. STATE OF ART FOR CP AND TCP: REMOVAL ALTERNATIVES

2.1. Physicochemical treatments

Different physicochemical technologies for the treatment of water, soil and sediments contaminated with CP and TCP have been studied. Among these are photodegradation in water by UV/H_2O_2, coagulation/flocculation, UV Fenton treatment, gamma radiation, photolytic and photocatalytic degradation, among others[27–33].

Of these, gamma rays showed the best results with a 100% degradation of 500 µg/L of TCP solution at an absorbed dose of 575 Gy with a rate of 300 Gy/h. Many of the treatments mentioned above have certain disadvantages, mainly economic, due to the high cost of the used materials [34]. Furthermore, studies have demonstrated that

advanced oxidation processes have the capability to generate potentially more toxic by-products, such as O- and S-trimethyl phosphates, as well as more toxic oxons [35,36]. Biological methods are reported in literature as practical remediation options. The use of microorganisms has emerged as an attractive option for the degradation of diverse types of pesticides[37,38]. In fact, microbial degradation is a safe, low-cost, and efficient method to clean up environments contaminated with diverse pollutants[2,37,39–42].

2.2. Biological treatments

Bioremediation of harmful complex recalcitrant compounds via microbes has been widely employed since microorganisms possess the ability to degrade them through successive enzymatic process into harmless simpler inorganic molecules. In fact, different microbes have the ability to utilize xenobiotic compounds like OPs or its derivatives as energy source by synthesizing the enzymes that degrade these compounds [19,42,43]. To date, several studies have been carried out to isolate microorganisms of different genera capable of biodegrading CP and TCP at different concentrations. Some of these microorganisms are shown in Table 4.

Table 4. Strains used for the biodegradation of CP and TCP.

Name	Organisms	Sample isolated from	[CP]	[TCP]	% of degradation	Reference
DT1	*Cupriavidus* sp	soil	100 mg/L;	100 mg/L	CP: 100% in 6h; TCP: 100% in 30 days	7
DSP3	*Alcaligenes faecalis*	soil	100 mg/L	100 mg/L	CP: 100% TCP: 93.5% both in 12 days	44
B14	*Enterobacter*	soil	25 mg/kg	-	40% in 48h	45
T6	*Ralstonia* sp	Active sludge		700 mg/L	100% in 80h	46
C2A1	*Bacillus pumilus*	soil	1000 mg/L;	300 mg/L	CP: 89% in 15 days; TCP: 90% in 8 days.	47
GFRC-1	*Acremonium* sp	laboratory-enriched red agricultural soil	300 mg/L	-	83.9% in 20 days	48

Table 4. (continued)

Name	Organisms	Sample isolated from	[CP]	[TCP]	% of degradation	Reference
KR100	*Burkholderia* sp	paddy soil	-	300 µg/ml	89.8% in 168h	49
TRP	*Paracoccus* sp	Active sludge	50 mg/L	50 mg/L	100% in 4 days	50
HM01	*Arthrobacter* sp	soil	100 mg/L	-	99% in 10h	51
JAS2	*Ochrobactrum* sp	Paddy rhizosphere soil	300 mg/L	-	100% in 12h	52
MB497	*Bacillus thuringiensis*	Soil of agricultural fields	200 mg/L	28 mg/L	CP: 99% in 9 days; TCP: 90.57% in 72h	52
JAS3	*Sphingobacterium* sp	Paddy field soil	300 mg/L	-	100% in 5 days	53
C1B	*Sphingobacterium* sp	Apple orchard	35 mg/L	-	100% in 14 days	54

Despite pure microbial strains have bioremediated CP and TCP, the utilization of pure cultures does not accurately represent the bioremediation process under natural environments. [55]. The use of microbial consortium can be more efficient in the degradation of OP pollutants than a single-strain culture because the consortium possesses many organo-phosphorus-related enzymes that can participate in the contaminant's complete mineralization and avoid the accumulation of toxic intermediate metabolites[39,56]. Despite these benefits, just a few studies have explored the use of consortia to biodegrade CP and TCP.

One of these studies was the one carried out by John et al., in 2016, in which they used a consortium of bacteria that included *Staphylococcus warneri* CPI2, *Stenotrophomonas maltophilia* CPI 15, and *Pseudomonas putida* CPI 9 for the degradation of CP. Their findings demonstrated that this consortium was able to degrade 96% of the CP initial concentration (125 ppm) within a timeframe of 8 days, under standard conditions of temperature and pH (30°C and neutral pH). [57].

Zhang et al. in 2018 used three groups of anaerobic reactors packed with zero valent iron (mono-ZVI system), ZVI coupled with anaerobic sludge (coupled system) and anaerobic sludge (mono-cell system) to degrade CP and TCP. Among the microorganisms that participated in this process, the genera *Pseudomonas, Zoogloea*, the phyla of Acidobacteria, Bacteroidetes, Chloroflexi, Proteobacteria, among others, were reported. This study began with a CP concentration of 800 µg/L of which, after the first week of operation, removals of up to 95% were obtained. For TCP removal, this study showed residual concentration of TCP of 30 and 53 µg/L in the coupled and mono-cell system after 29 and 33 days, respectively. Nevertheless, decrements in TCP degradation levels and increments in its concentration were noticed after 7 days of exposure.

In the same year, Abraham, J. & Silambarasan, S. used a fungal consortium which were isolated from paddy field soil to degrade CP and TCP. The study was developed in mineral medium and soil with fungus JAS1 and JAS4 strains. The

fungal consortium was spiked with 300 mg/L CP and degraded it completely within 12 h of incubation in the mineral medium along with TCP. Two experiments were carried out in soil. In the first one, the fungal consortium was added with nutrients (i.e., carbon, nitrogen, and phosphorous), and the second one lacked them. In both experiments, CP (300 mg/kg soil) and TCP were degraded within 24h and 48 h, respectively[58].

In 2019, Wang, S. *et al*., investigated the TCP biodegradation in dryland soil under anaerobic conditions. The experiment involved incubating a dryland soil contaminated with CP to develop a microbial consortium capable to degrade TCP. The degradation of TCP was assessed by measuring the production of chloridion and CO_2. The researchers proposed the metabolic degradation pathway of TCP and identified key bacteria involved in its biodegradation. Their results showed that the enrichment cultures of dryland soil were able to metabolize 97% of TCP (100 mg/L) within a 20-hour period. The degradation pathway analysis revealed that both microbial and photolytic degradation processes were involved in the TCP degradation. Furthermore, under anaerobic conditions, reductive and hydrolysis dechlorination mechanisms played a role. The bacterial taxonomic analysis identified *Ochrobactrum* and *Delftia* as the dominant genera of bacteria involved in the biodegradation of TCP. [59].

More recently, *in 2020,* Sun, X. *et al.* adapted an activated sludge from an OP pesticide factory under long-term (20 weeks) CP stress to develop a microbial consortium for effective biodegradation of CP and TCP. Bacterial communities with different adapting periods were analyzed by high-throughput sequencing. The microbial consortium MC-BSPK was composed of *Bacillus* sp. MC-B, *Serratia* sp. MC-S, *Pseudomonas* sp. MC-P, and *Klebsiella* sp. MC-K. Under optimized degradation conditions (pH 8.0 and 31 °C), the consortium exhibited remarkable biodegradation capabilities and achieved complete degradation of CP (50 mg/L) within 9 days and 88.6% degradation of TCP (50 mg/L) within 15 days. In 2021, Uniyal, S. *et al*., formed the consortium ECO-M by isolating the CP degrading bacterial strains viz *Agrobacterium tumefaciens* strain ECO1, *Cellulosimicrobium funkei* strain ECO2, *Shinella zoogloeoides* strain ECO3, and *Bacillus aryabhattai* strain ECO4 from the CP-contaminated agricultural soil of the Indian Central Himalaya. At an initial CP concentration of 50 mg/L, 30°C,

and inoculum of 10% (v/v), the microbial consortium ECO-M degraded 100% of CP concentration within 6 days. The subsequent degradation of TCP and 2-hydroxypyridine were confirmed by GC-MS analysis[61].

Even the use of microbial consortium has demonstrated capacities to degrade a wide range of CP and TCP concentrations under different conditions, the time it takes to achieve a complete degradation highly varies from hours to days [24,41,68,69]. On this regard, the use of metals with catalytic properties have been explored due to their potential to increase the rate of kinetics reactions[62].

2.3. Catalysts.

Due to of their physical and chemical properties, precious metals are widely used as catalysts in various industries, agriculture, and medicine. Among these, platinum group metals (e.g. platinum (Pt), ruthenium (Ru), palladium (Pd)) are widely applied as catalysts[63]. Besides, several reports on nanoparticles (NPs) (discrete particles with a size in the range of 1–100 nm) have revealed a remarkable catalytic performance in terms of selectivity, stable activity, and reactivity[64,65]. In fact, NPs hold great potential because they have particular physicochemical properties that differentiate them from bulk metals[65,66].

NPs can be synthesized by conventional chemical and physical methods. However, these methods utilize harmful and expensive chemical agents to reduce metal salts into their zerovalent metallic form. On the opposite to conventional methods, biological synthesis of NPs is an attractive choice for catalysts production[67,68]. While the use of microorganisms for remediation purposes has been practiced for many years, their application in NP synthesis is relatively recent.[69,70].

As shown in Table 5, the majority of studies have employed single strains of bacteria for NPs production. However, utilizing bacterial consortia offer several advantages over pure cultures such as reduced operational expenses, elimination of aseptic conditions, tolerance to toxic substances, adaptability to environmental changes

(e.g., temperature, pH, and redox potential), and facilitation of synergistic interactions among the consortium members. [71,72]

Table 5. Bacteria used to produce metallic NPs.

Bacteria	Metal NP	Reference
Desulfovibrio desulfuricans	Pd	73
Pseudomonas aeruginosa	Pd	74
Geobacter sulfurreducens	Pd	75–77
Shewanella algae	Pt	78
Desulfovibrio alaskensis G20	Pd, Pt	79
Rhodococcus sp.	Au	80
Morganella sp.	Ag	81
Klebsiella pneumonia	Ag	82
Enterobacter sp	Hg	83

A promising alternative for the reduction of water contaminants such as halogenated alkenes and aromatic compounds is the use of Pd-based catalysts[84]. Table 6 summarizes some of the characteristics that give Pd unique properties. Different studies have explored the use of metals such as Pt, copper (Cu), zinc (Zn), and niquel (Ni) for the catalytic reduction of various pollutants. However, Pd-based catalysts are more active, stable, and selective for obtaining the desired final products.

Furthermore, Pd can catalyze a wide range of reactions such as hydrogenation[85], hydrogenolysis[85,86], hydrodeoxygenation[64,87], hydrodehalogenation[88,89], among many others. This ability is given by the Pd affinity for hydrogen (H_2) and Pd exceptional adsorption capacity for this gas (900 times its own volume)[84,90]. In fact, the ability of metallic Pd to adsorb H_2, results in the creation of adsorbed surface H_2,

thereby enabling the activation of H_2 for the purpose of engaging in reduction reactions with coadsorbed substrates[64].

Table 6. Physico-chemical properties of Pd[91].

Symbol	Pd
Atomic number	46
Molecular weight	106.92
Block, group, and period	d, 10, 5
Oxidation state	+2, +4
Electronegativity	2.2
Density (20°C), g/cm^3	11.99
Ionization energies, kJ/mol	804.4, 1870, 3177
Melting point, °C	1554.9
Boiling point, °C	2963

Microorganisms can change the oxidation state of metals by redox reactions. For example, *Geobacter* sp and *Shewanella* sp have been widely explored for the synthesis of metallic NPs[68]. The microbial NP synthesis is commonly explained by their microorganisms capacity to reduce metals and to accumulate them in their elemental state. This process is facilitated by enzymes produced through cellular activity. This synthesis of NPs can be intracellular (if the NPs are formed inside the cell by transporting ions to its interior) or extracellular (by trapping metal ions on the cell surface)[70,92].

The use of pure strains to achieve Pd(II) reduction and Pd(0) recovery has been reported in several studies. *Shewanella oneidensis* and *Desulfovibrio desulfuricans* are the most analyzed microorganisms for their capacity to reduce Pd(II). Pd(II) reduction often happens under anaerobic conditions by using H_2 or ethanol as typical electron donors[93–96].

However, only a few studies have used microbial consortia for the synthesis of Pd NPs. One of these few studies was the one carried out by Pat-Espadas *et al.*[97] The

experiment used methanogenic granular sludge to reduce Pd(II) to Pd(0) in conjunction with the evaluation of different electron donors (i.e., formate, H_2, ethanol, acetate, lactate, and pyruvate) for their effectiveness in promoting Pd reduction. The batch reduction experiments consisted of the addition of 0.5 g VSS/L of anaerobic granular sludge, 25 mg of Pd(II)/L in form of Na_2PdCl_4 and a final concentration of 0.115 g chemical oxygen demand (COD)/L of the donors in both bioassays and in cell-free media assays. On one hand, their findings indicated that both formate and H_2 effectively facilitated the reduction of Pd, regardless of whether the process was chemically or biologically mediated. In contrast, ethanol only promoted Pd(II) reduction under biotic (biologically mediated) conditions. No reduction was observed in either biotic or abiotic (chemically mediated) assays with other tested electron donors, including acetate, lactate, and pyruvate.

In 2013, Martins *et al*.[98], enriched a consortium that contained *Desulfovibrio desulfuricans* and *Desulfobulbus rhabdoformis* with a sludge sample from a municipal wastewater treatment plant to evaluate its Pd (II) removal ability and its bio-recovery as NPs. The assays were performed in batch mode under anaerobic conditions supplemented with Pd(II) at range concentrations from 6 to 27 mg/L. This sulfate-reducing bacteria enriched consortium was able to reduce 60% of Pd(II) from aqueous solution after 13 days of incubation in the presence of 6 mg/L Pd(II) and after 6 days in the presence of 10 and 18 mg/L Pd(II). The community also achieved to reduce 43% of 26 mg/L Pd(II) in addition to reduce sulfate. Phylogenetic analysis of the 16S rRNA gene showed that this community was mainly composed of bacteria closely related to several *Clostridium* species and in a lesser extent by bacteria affiliated to genera *Bacteroides* and *Citrobacter.*

In a study conducted by Zhou et al. in 2016 [99], a bench-scale Membrane Biofilm Reactor (MBfR) was evaluated for its effectiveness to recover Pd(0) from a synthetic waste stream. The waste stream contained approximately 200 mg/L of soluble Pd(II). The researchers used anoxic sludge as the inoculum for the MBfR. They examined the reduction of Pd(II) and the microbial structure within the biofilm under steady states characterized by poorly- and well-buffered conditions. Results showed that at steady states, over 99% of the

soluble Pd(II) was reduced through enzymatic and autocatalytic processes at a pH range of 4.5 to 6.9. Regarding the bacterial community, they performed 16S rRNA gene sequencing and demonstrated that the dominant phylotypes potentially responsible for the reduction of Pd(II) were denitrifying β-proteobacteria mainly consisting of the family *Rhodocyclaceae*.

Even the use of microbial consortia for the reduction of Pd(II) is scarce, the recovery of Pd NPs by different microorganisms and bacterial consortia and their utilization for water pollutants reductive transformation have already been studied[64,100–103]. However, there are no studies of TCP removal by Pd NPs obtained from a bacterial consortium.

3. JUSTIFICATION

Due to its wide use worldwide, great solubility in water, its toxicity, and antimicrobial effect, TCP becomes prone to accumulate and spread in the environment, thus being able to cause various adverse effects to the population and ecosystem. Numerous approaches, both physico-chemical and biological, have been used for the treatment of this metabolite; however, several of these methods are associated with elevated operational expenses, the production of harmful by-products, or the need for aseptic conditions. The reduction of Pd(II) to Pd(0) driven by microorganisms is considered a viable alternative for the reductive transformation of various contaminants due to its properties as biocatalyst. Therefore, the use of Pd NPs synthesized by a microbial consortium is presented as a promising alternative for the reduction of TCP.

4. HYPOTHESIS

The Pd NPs synthesized by a microbial consortium supplied with an inorganic (H_2) and organic (glucose) electron donor would catalyze the reduction of TCP. H_2 would foster both abiotic and biotic Pd and TCP reduction experiments. The presence of fermenters in the inoculum in the glucose-amended consortia could facilitate the reduction of Pd. Herein, the reduction of TCP by using glucose will proceed similarly regardless of the presence or absence of Pd NPs, due to the existence of fermenters which could play a crucial role in facilitating the production of biohydrogen. The microbial communities would be diverse and some expected genera to find in the TCP-microcosms are *Pseudomonas* sp*., Bacillus* sp*., Klebsiella* sp*., Enterobacter* sp*.,* and *Acinetobacter*.

5. OBJECTIVES

5.1. General

Comprehend the catalytic role of Pd NPs synthesized by a bacterial consortium in the reduction of TCP.

5.2. Specifics

- Analyze the capacity of anoxic sludge to reduce Pd(II) in the presence of two suitable electron donors.
- Characterize the Pd NPs obtained by scanning electron microscopy and energy-dispersive X-ray spectroscopy analysis to observe differences in the content of Pd in the abiotic and inoculated microcosms depending on the used electron donor.
- Evaluate the effect of the Pd-enriched anoxic sludge as a catalyst to achieve the reduction of TCP.
- Identify the microbial groups associated with TCP biodegradation to elucidate the communities' diversity and structure between the different systems (i.e., inorganic and organic microcosms) by using next generation sequencing.

6. MATERIALS AND METHODS

6.1. Source of sludge

The sludge was obtained from the anoxic zone at a local wastewater treatment plant (WWTP) Agua Tratada del Potosí, S.A. of C.V (Figure 2). Numerous studies have shown the capacity of anoxic sludge to achieve Pd reduction and NPs production by providing a suitable electron donor to remove and/or biotransform different kinds of water contaminants[104–107].

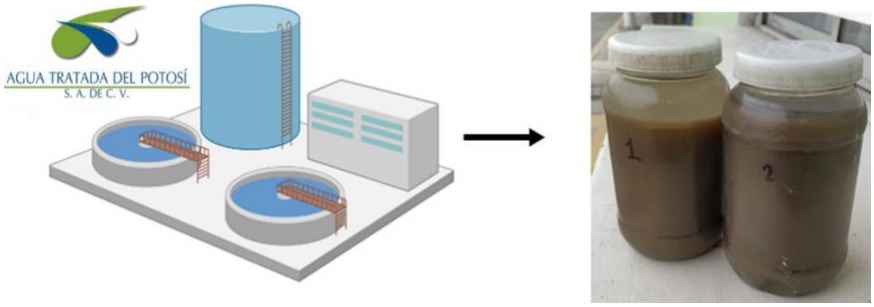

Figure 2. Anoxic sludge collected from WWTP Agua Tratada del Potosí, S.A. of C.V.

The anoxic sludge was characterized in regards total solids (TS), total suspended solids (TSS), and volatile suspended solids (VSS). Measurements were carried out by triplicate samples according to standard methods (2540-B and 2450-E) (APHA/AWWA/WEF, 2012). Table 7 shows sludge characterization. The anoxic sludge was stored at 4°C before use as inoculum for the microcosms.

Table 7. Solid characterization values (g/L)

TS	TSS	VSS
6.64 ± 0.56	5.54 ± 0.08	4.48 ± 0.07

6.2. Batch Pd(II) reduction experiments

Pd(II) reduction experiments were performed in 120 ml serological bottles covered with inert stoppers with a final volume of 80 ml of synthetic medium. The mineral medium used (modified from Chung et al., 2006) consisted of (g/L): KH_3PO_4 0.0128, Na_2HPO_4 0.0434, $NaNO_3$ as N 0.00607, $CaCl_2*2H_2O$ 0.001, $FeSO_4*7H_20$ 0.001, $MgCl_2$ 0.0034; and 1 mg/L trace mineral solution. The trace mineral solution (mg/L) consisted of: $ZnSO_4*7H_2O$ 100, $MnCl_2*4H_2O$ 30, H_3BO_3 300, $CoCl_2*6H_2O$ 200, $CuCl_2*2H_2O$ 10, $NiCl_2*6H_2O$ 10, $Na_2MoO_4*2H_2O$ 3 and Na_2SeO_3 30. Sulfate was limited in the medium to avoid interference with Pd, since it can precipitate as PdS. The synthetic media was autoclaved before its inoculation in a laminar flow chamber. Serological bottles were inoculated with flocculent anoxic sludge to produce a concentration of 0.5 g SSV/L. Subsequently, the liquid and the head space were pressurized with N_2 to avoid the presence of atmospheric oxygen.

Five different microcosms named NPs-Biotic H_2 (NPs-BH), NPs-Abiotic H_2 (NPs-AH), NPs-Biotic Glucose (NPs-BG), NPs-Abiotic Glucose (NPs-AG) and NPs-Donor Control (NPs-DC) were configured (Table 8). Depending on the microcosm configuration, glucose (2 g COD/L) or H_2 (at a final headspace pressure of 1 atm) were provided as electron donor. Finally, Pd(II) was provided to each microcosm in

the form of Na_2PdCl_4 to give a final concentration of 20 mg Pd(II)/L. All experimental treatments were established in triplicate and were incubated at 30 °C for 24 h[108].

Table 8. Microcosms setup for Pd(II) reduction experiments.

Microcosms	Synthetic medium	Anoxic sludge	Pd(II)	H_2	Glucose
NPs-BH	✓	✓	✓	✓	**X**
NPs-AH	✓	**X**	✓	✓	**X**
NPs-BG	✓	✓	✓	**X**	✓
NPs-AB	✓	**X**	✓	**X**	✓
NPs-DC	✓	✓	✓	**X**	**X**

6.3. TCP reduction experiments

Anoxic sludge enriched with Pd was tested as a biocatalyst to achieve TCP reduction. TCP stock solution (100 mg/L) was prepared in mineral medium and stored at 4°C before use. Subsequently, TCP was taken from the stock solution to give a final concentration of 10 mg/L for the seven types of microcosms. These microcosms were referred to as TCP-H_2-coupled, TCP-H_2-no catalyst, TCP-H_2-abiotic, TCP-G-coupled, TCP-G-no catalyst, TCP-G-abiotic, and TCP Donor control (TCP-DC). The compositions of the different microcosms are shown in Table 9.

The microcosms were covered with aluminum foil and incubated in the dark to prevent photodegradation of TCP. All experimental treatments were established in duplicate and incubated at 30 °C for 24 h. Samples were analyzed at specific time intervals that were determined before final experimentation to monitor the change in TCP concentration.

Table 9. Microcosm setups for TCP reduction experiments.

Microcosms	Synthetic medium	Anoxic sludge	Pd(II)	TCP	H_2	Glucose
TCP-H_2-coupled	✓	✓	✓	✓	✓	**X**
TCP-H_2-no catalyst	✓	✓	**X**	✓	✓	**X**
TCP-H_2-abiotic	✓	**X**	✓	✓	✓	**X**
TCP-G-coupled	✓	✓	✓	✓	**X**	✓
TCP-G- no catalyst	✓	✓	**X**	✓	**X**	✓
TCP-G-abiotic	✓	**X**	✓	✓	**X**	✓
TCP-DC	✓	✓	✓	✓	**X**	**X**

Where:

coupled= microbial consortia + Pd catalyst

no catalyst= lack of Pd catalyst

abiotic= lack of microbial consortia

6.4. Analytical techniques

The content of Pd(II) in the liquid samples was analyzed by Inductively Coupled Plasma Atomic Emission Spectroscopy (ICP-OES, Model 738 ES Varian Brand) after being filtered through 0.22 µm Millipore membranes.

To document the reduction of TCP, the samples were filtered through 0.22 µm Millipore membranes and analyzed by High Pressure Liquid Chromatography (HPLC). A ZORBAX C-28 column (4.6 x 250 mm) was used. The mobile phase was a mixture of 85% methanol and 15% water. The TCP peak was observed at a particular wavelength of 240nm. The calibration curve was linear in the range of 0.5

-12 mg/L. Headspace pressure in microcosms containing H_2 as electron donor was measured with a manometer (Model 407910, Extech Instruments Corporation, Massachusetts, USA) for different time intervals in a 24 h period.

6.5. Scanning electron microscopy

Samples from different assays were prepared for scanning electron microscopy (SEM) by following the procedure of *Espadas et al.*[108] Pellets were washed three times in deionized water and dehydrated through a graded ethanol series (i.e., 50, 70, 90, and 100%) and then immersed in hexamethyldisilazane for 5 min, air dried, and further coated with gold.

The images were collected on an FEI - FIB Dual Beam Helios Nanolab 600 with an X-Ray Energy Dispersive Spectrometry (EDS) system by utilizing a SUTW-Sapphire detector type with a resolution of 142.10 eV. SEM images were collected at 10 kV.

6.6. DNA extraction and microbial community analyses.

After 24 h of incubation, 1 ml per each of the inoculated samples was taken and placed in Eppendorf tubes to centrifuge them at 13 rpm for 10 min. Biomass pellets were collected and stored at -20 C to later proceed with DNA extraction. The extraction was conducted according to the instructions provided by the manufacturer QIAGEN DNeasy PowerBiofilm Kit (QIAGEN, USA).

DNA samples were stored at -20ºC until the bacterial community analysis was performed by MiSeq Illumina platform at the Genomics Core at Arizona State University. The DNA was used to amplify the V4 16S rRNA gene hypervariable regions with primers 515F GTGCCAGCMGCCGCGGTAA and 806R GGACTACHVGGGTWTCTAA designed by Caporaso *et al.* 2011 [109]. Amplicon libraries (390–400 bp length) were constructed by following the Earth Microbiome Project (http://www.earthmicrobiome.org/emp-standard-protocols/) protocol. The libraries were sequenced on the Illumina MiSeq platform and run by using the version 2 modul, with a paired-end read configuration of 2x250 cycles.

Taxonomic analysis was carried out by using the open-source software package Dada2 (v1.18.0)[110] in R (version 4.1.1). Taxonomic annotation was conducted by utilizing the Silva 138.1 database file[111]. The R Phyloseq library[112] was used to perform alpha and beta diversity analysis of the microbial communities.

6.7. Statistical analysis

Duplicates of each microcosm were used to determine the kinetic evolution of the Pd NPs' formation and the TCP reduction. Data were subjected to one way analysis of variance (ANOVA) and Tukey's test to compare means and determinate the significant difference between the experimental treatments at the 95% confidence interval. Analysis was performed using Minitab 17 Statistical Software (2010) for Windows. All plots were created using the graphing software OriginPro, 2016 (OriginLab Corporation, Northampton, MA, USA).

7. RESULTS AND DISCUSSION

7.1. NPs synthesis

Pd(II) reduction experiments were performed by preparing biotic and abiotic microcosms with H_2 or glucose as inorganic and organic electron donors. The objective was to achieve the synthesis of desirable Pd NPs for the reduction of the TCP contaminant. After taking samples for different time intervals in a 24 h period, the results obtained are shown in Figure 3.

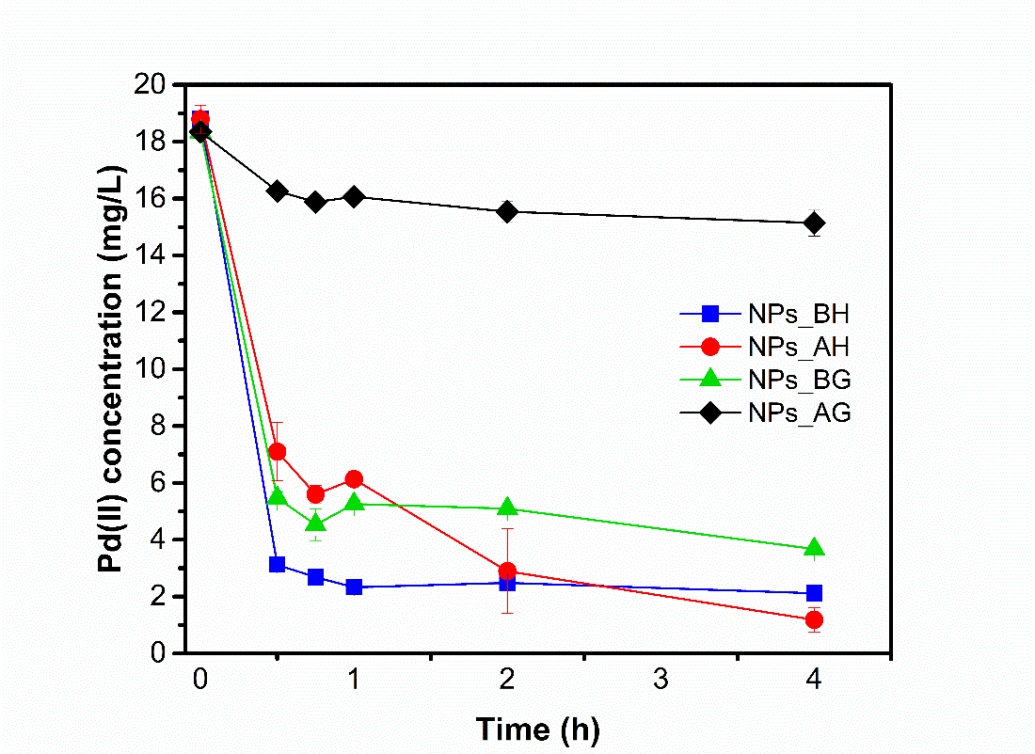

Figure 3. Kinetic evolution of Pd(II) reduction in biotic and abiotic microcosm supplemented with H_2 (■, ●) and glucose (▲, ◆). Where NPs-BH=NPs-Biotic H_2, NPs-AH=NPs-Abiotic H_2, NPs-BG= NPs-Biotic Glucose, and NPs-AG= NPs-Abiotic Glucose.

In microcosms with H_2 as electron donor, reduction of Pd(II) was observed in both biotic and abiotic assays. Figure 3 shows no significant differences between the concentration of Pd(II) in the NPs-BH and NPs-AH microcosms after two hours of incubation. In fact, there were not significant differences until the end of the experiment showing that the decrease in the concentration of Pd(II) does not require the presence of microbial biomass. After 24h, >95% of the soluble Pd was reduced and in parallel black materials appeared in the bottom of the inoculated and non-inoculated microcosms (Figure 4) which implies Pd(II) precipitation.[113].

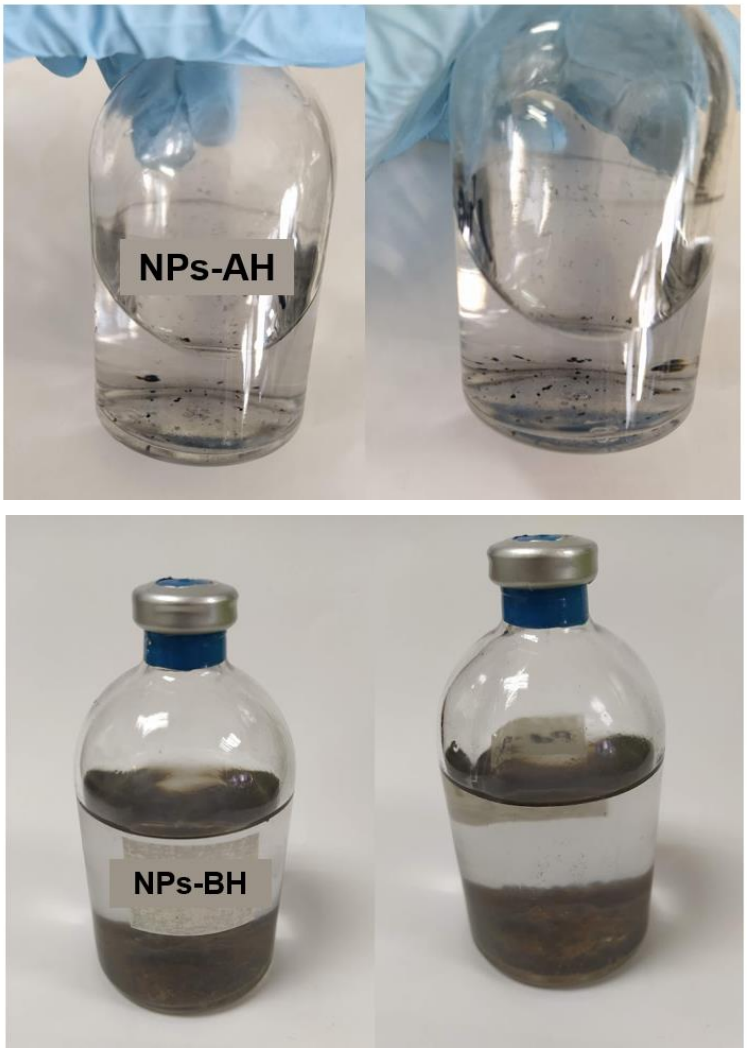

Figure 4. Black precipitates in the microcosms NPs-AH and NPs-BH

In regards to the black materials observed in the H_2-microcosms, Zhou *et al*. have shown similar results in their simultaneous microbial-driven and Pd-catalyzed nitrate reduction experiments. They employed three identical H_2-based membrane biofilm reactors (MBfRs) operated in parallel and inoculated with anoxic sludge from a WWTP. They continuously introduced 200 mg/L of soluble Pd (as Na_2PdCl_4) into the inoculated and non-inoculated reactor. Within 2 days, >99% soluble Pd was immobilized as black precipitates on the surface of the hollow membranes of both reactors. The formation of Pd NPs was confirm utilizing XRD, and showed the predominant presence of the Pd(0) crystal structure in both reactors[114]. Also, Zhou et al.[113], evaluated a bench-scale MBfR for its ability to recover Pd(0) from a synthetic

waste stream containing 200 mg/L soluble Pd(II). They examined Pd(II) reduction and removal along biofilm microbial structure at steady states of poorly- and well-buffered conditions. Approximately 81% and 90% of Pd(II) was reduced within 47 and 62 h, respectively. At the same time, black materials were also accumulated on the fibers over time which implies Pd(0) precipitation.

In the assays with glucose, microbial cells substantially increased Pd(II) reduction rate. NPs-BG and NPs-AG microcosms had significant differences ($p<0.5$) between them since 0.5 h. Similar studies that utilize organic electron donors such as acetate, pyruvate, lactate, or ethanol demonstrated the ineffectiveness of these chemicals to directly catalyze the reduction of Pd(II)[97]. However, a decrease in the Pd(II) concentration in the NPs-AG microcosm can be noticed, so it can be inferred that a cross contamination could have occurred. Individually, the NPs-BG microcosm does not present significant differences between 0.5 and 2 h, however a significant difference was detected at the end of the experiment. In fact, it had the highest percentage of Pd reduced after 24h of incubation (Table 10). In contrast, the NPs-AG microcosm did not present significant differences after 0.75 h and until 4 h.

Table 10. Pd(II) reduction kinetic values of the biotic and abiotic microcosms supplemented with H_2 (NPs-BH, NPs-AH) and glucose (NPs-BG, NPs-AG) at 24 h of incubation.

	20 mg Pd/L			
	NPs-BH	NPs-AH	NPs-BG	NPS-AG
% Pd reduced	95.09±0.89	95.70±0.49	99.59±0.49	45.52±6.28
Reduction rate (mg Pd/L-h)	0.74	0.75	0.76	0.35

Where: NPs-BH=NPs-Biotic H_2, NPs-AH=NPs-Abiotic H_2, NPs-BG= NPs-Biotic Glucose, and NPs-AG= NPs-Abiotic Glucose.

Figure 5-A and B shows samples of the aggregates from the different experiments that were analyzed by SEM-EDS. The conglomerates showed in the figures were

comprised of particles that exhibited a range of sizes between 50 and 15 nm, thereby providing concrete evidence of the presence of Pd NPs with H_2 and glucose as electron donors.

The abiotic controls showed aggregates rich in Pd which were consistent with the appearance of the black color precipitates formed at the bottom of the serological bottles (as seen in Figure 4). In fact, Pd(II) reduction was concomitant with the aggregates: the more time passed the more aggregates and minor Pd(II) concentration were observed.

H_2 can stimulate the spontaneous abiotic Pd(II) reduction and it can continue being reduced trhough autocatalysis in the presence of H_2 [113]. The rapid reduction of Pd(II) observed in this current study was chemically mediated and can be represented by equation 1:

$$Pd^{2+}(aq) + H_2(g) \rightarrow Pd(s) + 2H^+(aq) \qquad (1)$$

By contrast, Figures 5-C and D show the biotic microcosms which had dense aggregates and a random distribution, being tightly associated with microbial cells. These results are similar to those obtained from Pat-Espadas et al., 2016[100] where UASB granules exhibited a complex layer structure similar to those in this study, with craterous pores, and an outer layer composed of various types of bacteria with different shapes (e.g., cocci, bacilli). All those characteristics allowed the heterogeneous distribution of sites available for Pd(0) nucleation [97]. In fact, the presence of Pd precipitates in the surface of the bacterial cells suggests the possible microbial reduction of Pd(II) to Pd(0) followed a precipitation mechanism[115].

The Pd removal could occur through several mechanisms such as biosorption, bioaccumulation or an enzymatically driven mechanism, such as metal reduction and consequent precipitation[98]. Generally, Pd(II) microbial reduction with a suitable reductant, such as H_2, has been proposed to involve three concomitant steps: (i)

Pd(II) sorption to the cell, (ii) Pd(0) nucleation, and (iii) autocatalytic reduction of Pd(II) on the surface of Pd(0) nuclei[116].

Regarding the reduction of Pd(II) in the microcosm inoculated and supplied with glucose (Figure 5D), we can inferred the presence of fermentative bacteria. For example, some fermenters are used to produce biohydrogen[117–120], therefore, if glucose was fermented (e.g., alcoholic fermentation), one of the final products could have been H_2. This fermentatively produced H_2 could have been used as a reductant for Pd(II) reduction[68].

The presence of carbon, sodium, and calcium elements can be attributed to the microbial consortium or the components of the synthetic medium. Additionally, the elevated carbon percentage can be attributed to the utilization of conductive carbon adhesive tapes for sample mounting, while the presence of silicon may have originated from the supporting grid.

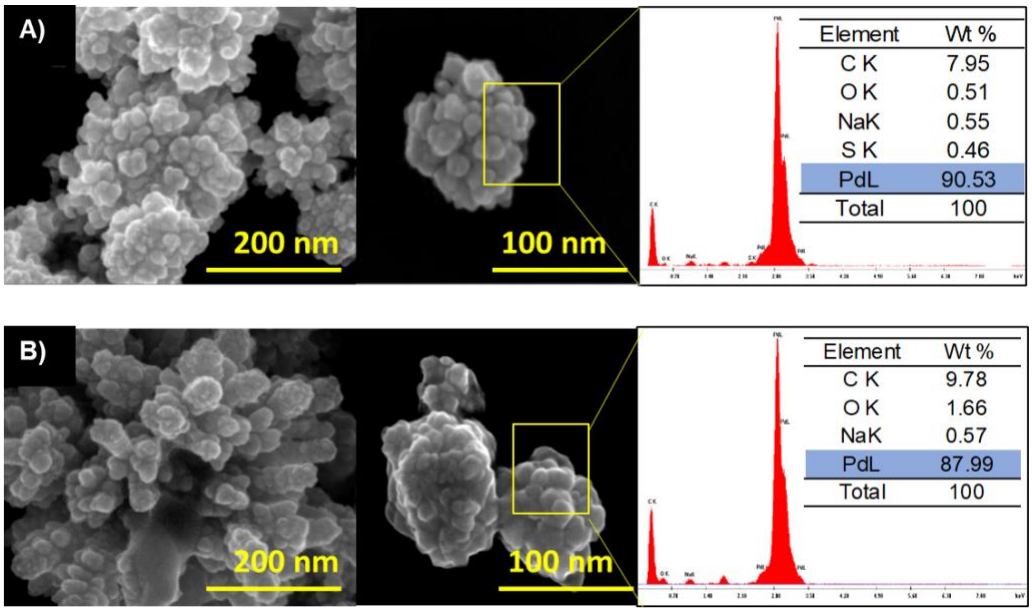

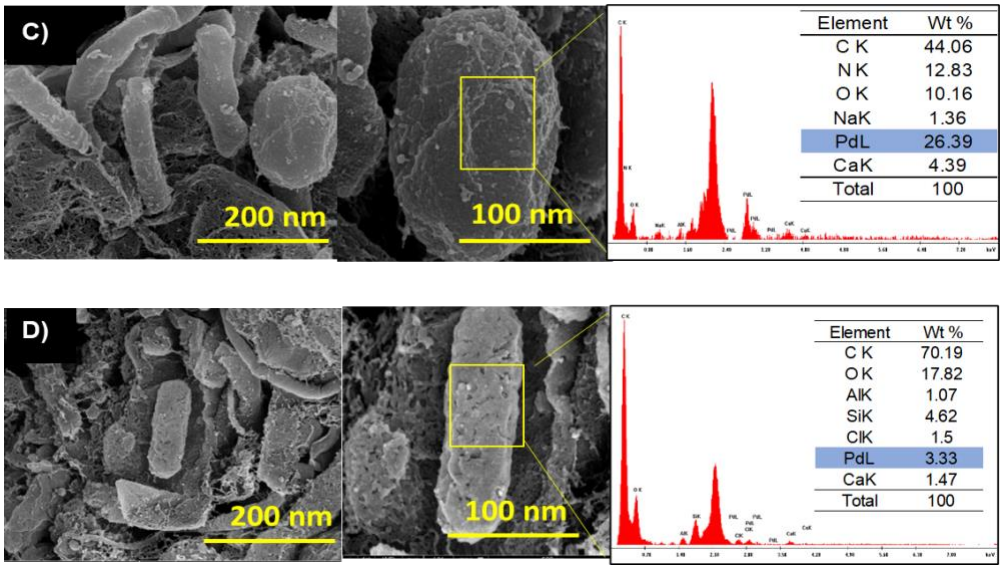

Figure 5. On the left, SEM images of Pd in the abiotic (A, B) and inoculated (C, D) microcosms supplemented with H_2 (A, C), and glucose (B, D). On the right, EDS analysis corresponding to the samples shown in the SEM images.

7.2. TCP reduction

According to the reduction kinetics of TCP that utilized H_2 as electron donor (Fig 6A), the microcosm that lacked a catalyst (TCP-H-no catalyst) did not present significant differences in the concentration of TCP, remaining at a concentration similar to the initial (9.46±0.30 mg TCP/L) until the end of the experiment. This high concentration of the contaminant in the medium is due to TCP's broad antimicrobial properties which makes it more difficult to reduce along with the absence of the catalyst Pd(0), which favors the reductive transformation of various contaminants including OPs[64,121]. It should be noted that the incubation of the different microcosms that utilize H_2 as electron donor to reduce TCP lasted 24 h (Table 11). However, no significant differences were found after 6 hours of incubation in all of the experiments.

On the contrary, the microcosm TCP-H-coupled and the one without inoculum (TCP-H-abiotic) showed significant differences from the beginning to the end of their incubation. Regardless that different bacterial species have reduced Pd(II) to Pd(0) to degrade recalcitrant pollutants[71,101], the abiotic microcosm achieved >95% reduction of TCP. This can be explained as H_2 can be used as reductant to convert dissolved Pd(II) ion to zero-valent Pd NPs through self-catalyzed reduction[122]. Pd NPs are effective because they strongly adsorb H_2 and activate it to reactive H_2 atoms on the NPs surface[90,123]. The reactive H_2 atom is useful for reducing a wide range of contaminants[84], such as TCP in this case.

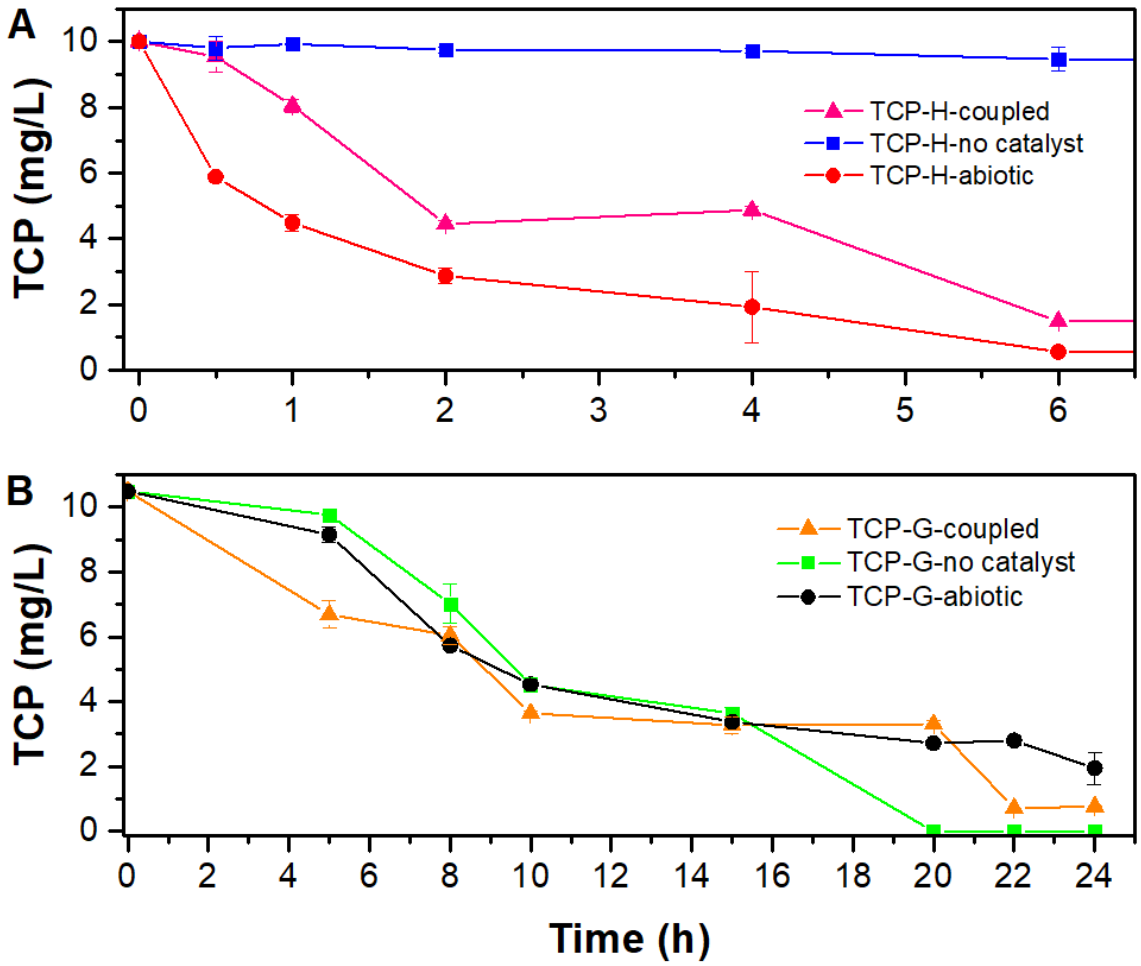

Figure 6. TCP reduction kinetics in the microcosms supplemented with H_2 (A) and glucose (B). Where, coupled= microbial consortia + Pd catalyst, no catalyst= lack of Pd catalyst, abiotic= lack of microbial consortia.

Regarding the microcosms with glucose as electron donor (Figure 6B), in all of them the reduction of TCP was successfully achieved. The TCP-G-Abiotic could reduce more than 80% of TCP within 24 h. This indicate that a sufficient amount of NPs was formed to achieve the reduction of the contaminant. As mentioned before, a possible cross contamination is inferred in the abiotic microcosm. A similar result was obtained from Pat-Espadas et al., [97] who employed various electron donors to examine the kinetic changes in Pd removal by anaerobic granular sludge in both inoculated and abiotic assays. The abiotic control with formate as the electron donor demonstrated a reduction rate of 53.22 ± 0.54 mg Pd/L-h. Additionally, the product resulting from this experiment was analyzed by XRD (X-ray diffraction), and the findings confirmed the formation of Pd(0), which indicated the successful Pd reduction.

For this part, the microcosm which contains biomass and the catalyst (TCP-G-coupled), achieved more than 90% of TCP reduction in 22 h. This result was expected since various studies have shown that different bacterial species are capable of synthesizing Pd NPs when a suitable electron donor is available and using these NPs as catalysts for the degradation of recalcitrant contaminantss[124–126].

The microcosm that lacked Pd, TCP-G-no catalyst, managed to reduce t100% of TCP in the medium at 20 h and achieved the maximum reduction rate (Table 11) of all the microcosms. TCP-G- no catalyst microcosm stopped presenting significant differences after 20 h, from that moment the contaminant was no longer detected. Despite of the catalyst's lack in this microcosm, the addition of the inoculum allowed bacteria to efficiently reduce TCP because of their wide range of enzymes. Those enzymes present in the microorganisms handle degradation in a process call enzymatic degradation[127]. During enzymatic degradation, the xenobiotic compound enters the microbial cells and undergoes a series of biochemical and physiological reactions, which include oxidation, reduction, hydrolysis, condensation, or dehalogenation. As a result of these reactions, the xenobiotic is transformed into either nontoxic metabolites or completely mineralized, rendering it harmless to the environment.[19].

It is important to note that during the analysis of the samples by HPLC, the observation of potential formation of additional compounds was made in the microcosms supplemented with glucose. Other unknown peaks were detected by HPLC starting from 5 hours of incubation, and this trend continued thereafter. Many studies employing an organic donor have proposed the degradation pathway of TCP to involve sequential dechlorination steps, leading to the cleavage of the pyridine ring and eventual complete mineralization of the contaminant[19,128]. Therefore, the compounds observed in the HPLC analysis could potentially represent one of these degradation products. Conversely, in the systems containing H_2, formation of additional compounds was not observed.

The degradation mechanism can be broadly described in three stages. First, the target xenobiotic experiences adsorption at the microbial cell membrane. Second, the xenobiotic enters the microbial cell by crossing the cell membrane. The rate and efficiency of this process depend on the xenobiotic's molecular. Finally and once inside the microbial cell, a series of enzymatic reactions take place and result in the transformation of the xenobiotic into either nontoxic compounds or complete mineralization. Additionally, the resulting metabolites may undergo further degradation through co-metabolism, contributing to the overall removal of the xenobiotic from the environment.

In addition to enzymatic degradation, the process of dechlorination can play a significant role in the degradation of TCP. TCP is initially utilized by microorganisms as an energy source. However, the removal of chlorine atoms from TCP can have a negative impact on the growth rate of microorganisms.

Certain microorganisms dechlorinate TCP by oxidizing the ortho and para-chlorine atoms, resulting in the formation of 3,6-dihydroxypyridyl-2,5-diketone. This oxidation process is a key step in the dechlorination pathway. Furthermore, certain species of fermentative bacteria have the capacity to produce H_2 during the fermentation process when glucose or similar organic donors are provided. This H_2 production

can subsequently participate in the reduction of Pd(II) to Pd(0), contributing to the overall degradation process.

Generally, the catalytic reduction of several water contaminants can be categorized into three main pathways: hydrodeoxygenation for oxyanions, N-N hydrogenolysis for N-nitrosamines, and hydrodehalogenation for halogenated organics[64]. The latter pathway involves the substitution of one or more carbon-bound halogen atoms with atomic hydrogen and is applicable to all halogenated compounds. However, in the context of halogenated aromatic compounds, the reduction in the aqueous phase of these diverse compounds typically follows a sequential dechlorination process[19,64]. It has been observed in various studies that, when multiple halogens are present, the less sterically hindered halogens tend to be removed first. Moreover, when H_2 is utilized as the electron donor, aromatic ring hydrogenation has been observed to occur afterwards the dehalogenation process.

Table 11. TCP reduction kinetic values of the different microcosms supplemented with H_2 and glucose after 24h of incubation

	10 mg TCP/L					
	TCP-H-coupled	TCP-H- no catalyst	TCP-H-abiotic	TCP-G-coupled	TCP-G- no catalyst	TCP-G-abiotic
% TCP reduced	82.70±0.72	5.39±3.05	96.49±0.46	92.68±0.01	100±0.00	81.49±4.03
Reduction rate (mg TCP/L-h)	0.34	0.02	0.40	0.41	0.44	0.36

Where:
coupled= microbial consortia + Pd catalyst
no catalyst= lack of Pd catalyst
abiotic= lack of microbial consortia

7.3. Microbial community structure and diversity

The phylogenetic sequencing data showed that all microcosms' communities were diverse. Figure 7 shows the main bacterial genera of the inoculated microcosms that were involved in Pd(II) and TCP reduction.

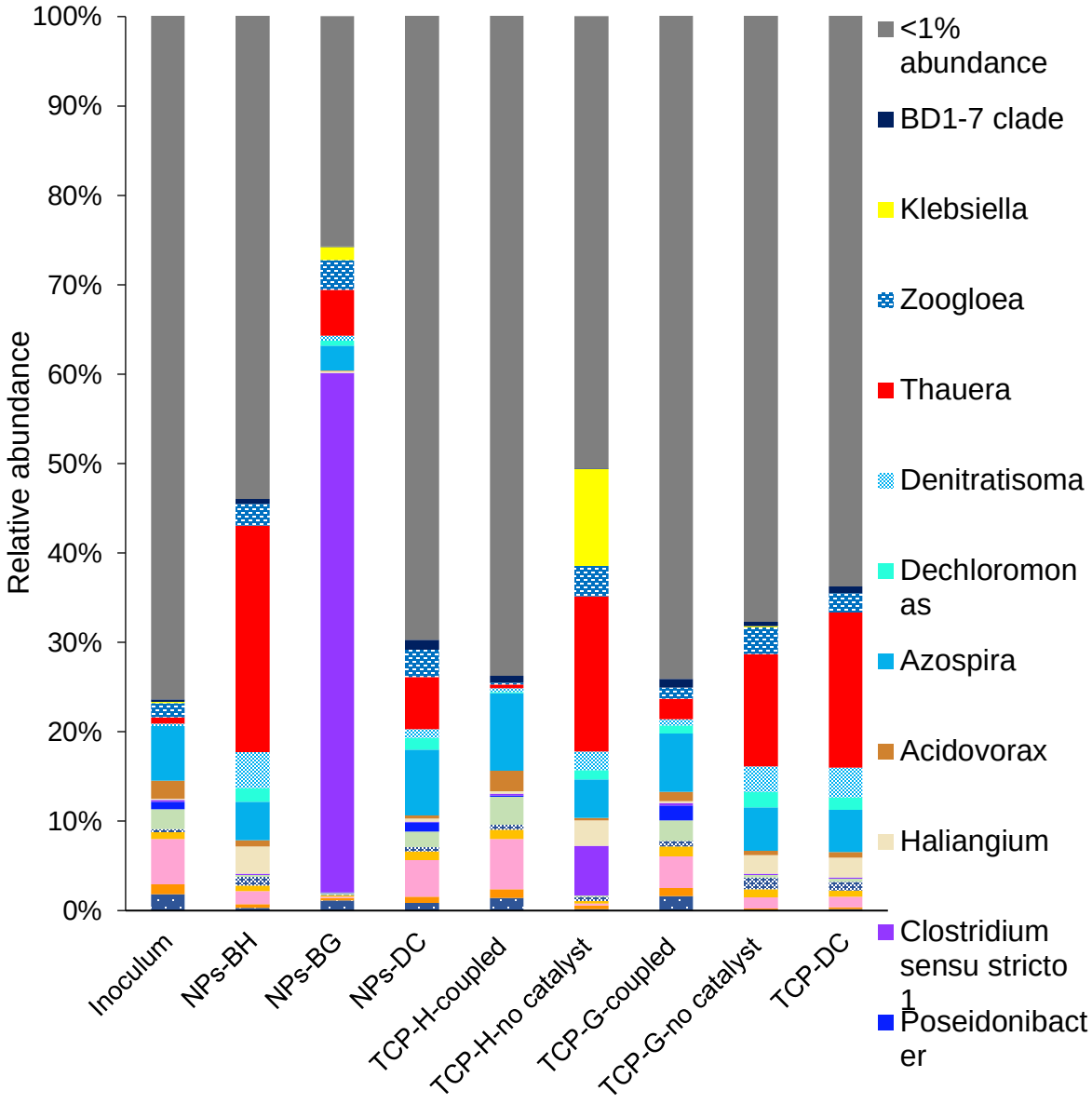

Figure 7. Relative abundances of phylotypes at the genus level for all the inoculated microcosms. All phylotypes (less than <1% relative abundance) are grouped and shown in gray. Where NPs-BH=NPs-Biotic H_2, NPs-BG= NPs-Biotic Glucose, and NPs-DC= NPs-Donor control; coupled= microbial consortia + Pd catalyst, no

catalyst= lack of Pd catalyst, abiotic= lack of microbial consortia and TCP-DC= TCP without electron donor.

Irrespective of the presence or absence of the electron donor and the contaminant TCP, the phylum Proteobacteria, specifically the genus *Azospira* was present in all the microcosms. Proteobacteria, comprises a diverse range of anaerobic, facultative, and aerobic bacteria, which have been associated with TCP and OP pesticides removal [129,130]. They are well-known for their significant role in key anaerobic steps such as acetogenesis, and their ability to utilize a variety of organic substrates to produce volatile fatty acids [121,129,130]. In fact, in the inoculum, *Azospira* represented the highest percentage of abundance, followed by the phylum Saprospiraceae at the genus level *OLB8*, with 6.11% and 5.09% abundance, respectively.

The abundance of other genera was less than 2%. It has been confirmed in various studies that *Pseudomonas* and *Acinetobacter* can degrade CP or TCP [131]. However, *Beutenbergia* was the only representative of the phylum Acinetobacter and had no more than 2% relative abundance in all the microcosms (maximum relative abundance of 1.81% in the inoculum).

In the NPs' microcosms, the NPs-DC (microcosms without H_2 or glucose as electron donor) also had a higher abundance of the phylum Proteobacteria, with the genera *Azospira* (7.39%) and *Thauera* (5.86%). These results were similar to those of the NPs-H microcosm, in which the genus *Thauera* (25.35%), followed by *Azospira* (4.31%), and *Denitratisoma* (4.01%) were dominant. Isolates of *Thauera* can utilize aromatic compounds and organic substrates such as sugars as electron acceptors, and they are frequently detected as important denitrifiers in biological systems and in some WWTP[129,132].

In contrast, the NPs-G microcosm presented a higher abundance of the phylum Firmicutes, and at the genus level *Clostridium sensu stricto 1* had 58.07% relative abundance. The phylum Firmicutes includes the main hydrogen-producing microorganisms, which can utilize various substrates such as glucose to produce H_2

[130]. The genus *Clostridium* generally consists of monospore-forming, anaerobic, Gram-positive-staining rods, and it has been reported as being capable to utilize glucose as an electron donor to reduce Pd(II) because of its tolerance to this metal, and to produce H_2 through fermentation[68]. This can further serve as an electron donor for the catalytic activity of the Pd(0) [68,98,133–135]. The second most abundant genus in NPs-G microcosm was *Thauera* (5.10%) followed by *Zoogloea* (3.37%), another member of the phylum Proteobacteria which is famous for producing glue-like extracellular polymeric substances (EPS) and binding cells together, a vital process for sludge granulation[121]. Furthermore, it is widely believed that this microorganism plays a significant role in denitrification processes WWTPs, given that *Zooglea* is a denitrifying bacteria frequently detected in WWTPs [136]

In the TCP microcosms, specifically in the donor control TCP-DC and the TCP-G-no catalyst, there was a higher percentage of *Thauera* and *Azospira*, similar to the NPs-DC and NPs-H microcosms. Despite having different electron donors, the phylum Proteobacteria specifically the genus *Azospira* and the phylum Bacteroidota, with the genus *OLB8* had the highest abundance in the TCP-H-couped and TCP-G-coupled. Bacteroidetes are proteolytic bacteria that have been involved to the degradation of various proteins and the mineralization of amino acids to produce volatile fatty acids such as acetate and propionate [137]. The TCP-H-no catalyst, which lacked Pd(II), had the highest percentage of the genera *Thauera* and *Klebsiella* from the Enterobacteriaceae family, which have been found in dark fermentation processes[137]

Although the genus *Clostridium Sensu Stricto 1* was the most abundant in the NPs-G-coupled due to its ability to utilize organic donors such as lactate and glucose to reduce Pd(II) to Pd(0), its relative abundance in the TCP-G- coupled and TCP-G-no catalyst was less than 1%. This can be attributed to the inhibitory effects of TCP on microorganisms [131]. Additionally, the presence of *Thauera* in the microcosms TCP-H-coupled and TCP-H-no catalyst decreased in comparison to the NPs-H-coupled which did not have TCP. This evolution of the bacterial consortium can be explained by the TCP antimicrobial effects.

The microbial diversity of all microcosms was studied by means of calculating Alpha (α) and Beta diversity. The α-diversity, characterized by the Chao1, Shannon, and Simpson indexes, summarizes the distribution of species abundances, and measures the overall community heterogeneity. Conversely, beta diversity serves to compare diversity between the microbial communities.

Figure 8 illustrates the phylogenetic diversity in terms of the Chao1, Shannon, and Simpson diversity indexes. Chao1 is a non-parametric estimator that estimates the number of species in a community. As depicted in Figure 7, the TCP-G-coupled, which contained glucose, TCP, and Pd(II), displayed the highest number of species, followed by TCP-DC. Notably, it has been reported that certain bacterial species can effectively utilize TCP as the sole source of carbon and nitrogen, which are primarily employed for cell growth and product formation [19,138]. In contrast, the NPs-G microcosm exhibited the lowest number of species, with the genus *Clostridium* sensu stricto being the most abundant species in this microcosm, representing more than 50% of the relative abundance.

A higher Shannon and Simpson index is indicative of greater microbial diversity. Concerning the Shannon index, the TCP-G-coupled exhibited the highest value among all samples. Excluding the NPs-G microcosm, which had a Shannon index value of 2.5, all other microcosms displayed values higher than 4. The Simpson's Diversity index measures the diversity by considering the number of species present, as well as the relative abundance of each species, and thus reports on the even distribution of microbial species. According to Figure 8, the microcosm TCP-G-coupled had the highest Simpson value among all other microcosms, meaning that this microbial community was evenly distributed and did not show a clear dominance by some genera such as in the case of NPs-G-coupled. Indeed, all the other microcosms had Simpson index values ~ 0.9, the NPs-G was the only one with a value under 0.7 This low value in the NPs-G microcosm, composed of synthetic medium, Pd(II), glucose and the inoculum, may indicate some toxicity from Pd(II) for the majority of the bacterial species. NPs-G showed a clear dominance by

Clostridium sensu stricto 1, and was the microcosm with a poor distribution of microbial strains.

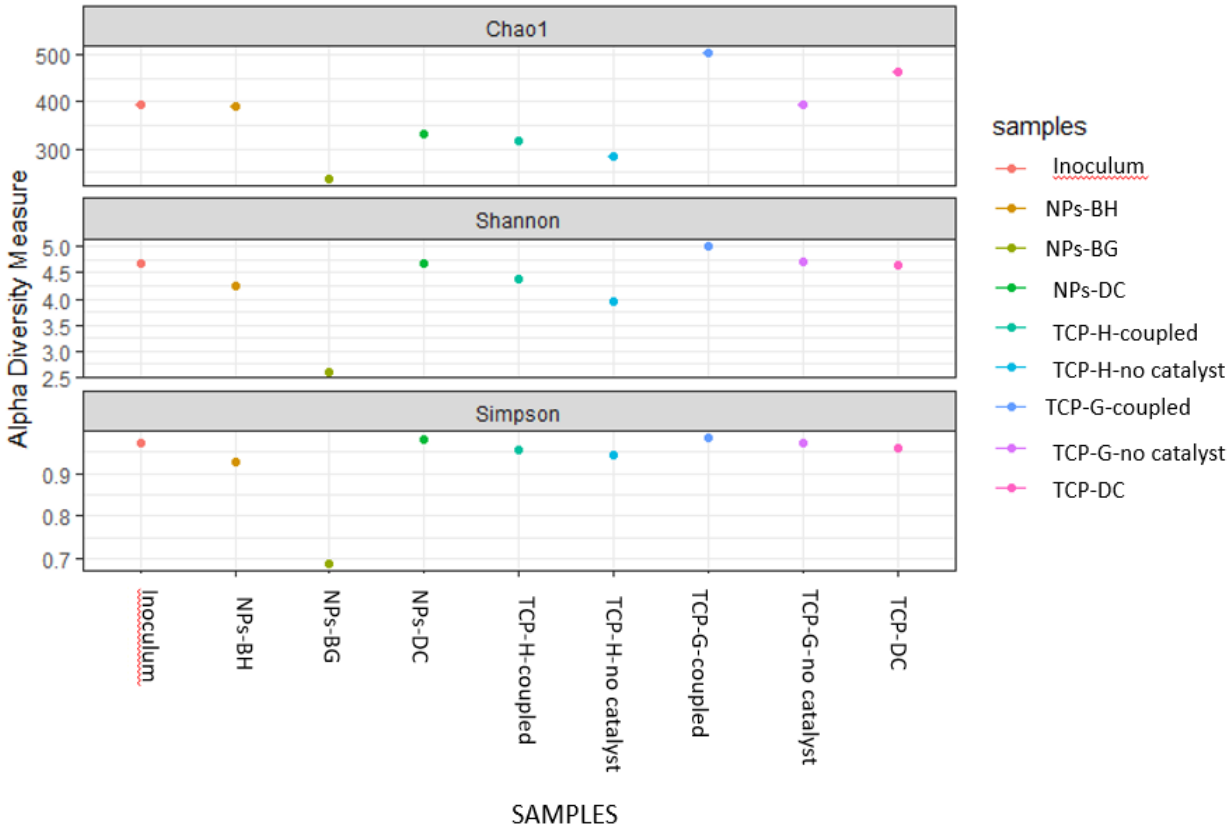

Figure 8. Alpha diversity indexes for all microcosms. Where NPs-BH=NPs-Biotic H_2, NPs-BG= NPs-Biotic Glucose, and NPs-DC= NPs-Donor control; coupled= microbial consortia + Pd catalyst., no catalyst= lack of Pd catalyst, abiotic= lack of microbial consortia and TCP-DC= TCP without electron donor.

Figure 9 shows the beta diversity analysis that addressed the microbial communities' changes among the different microcosms. From Figure 8, we observed four clusters: 1) Inoculum, NPs-DC, TCP-G, TCP-H, 2) NPs-H, TCP-DC, TCP-G-BC, 3)TCP-H-BC and, 4)NPs-G. The addition of the electron donor and TCP to the microcosms didn´t clearly separated the microbial communities. Only the third (TCP-H-BC) and fourth cluster (NPs-G) were certainly separated from the other microbial

communities. This is likely as NPs-G presented the major percentage of *Clostridium senso Stricto 1* and the TPC-H-BC had the major percentage of *Klebsiella.* The rest of the microcosms presented similar relative abundances of dominant phylotypes.

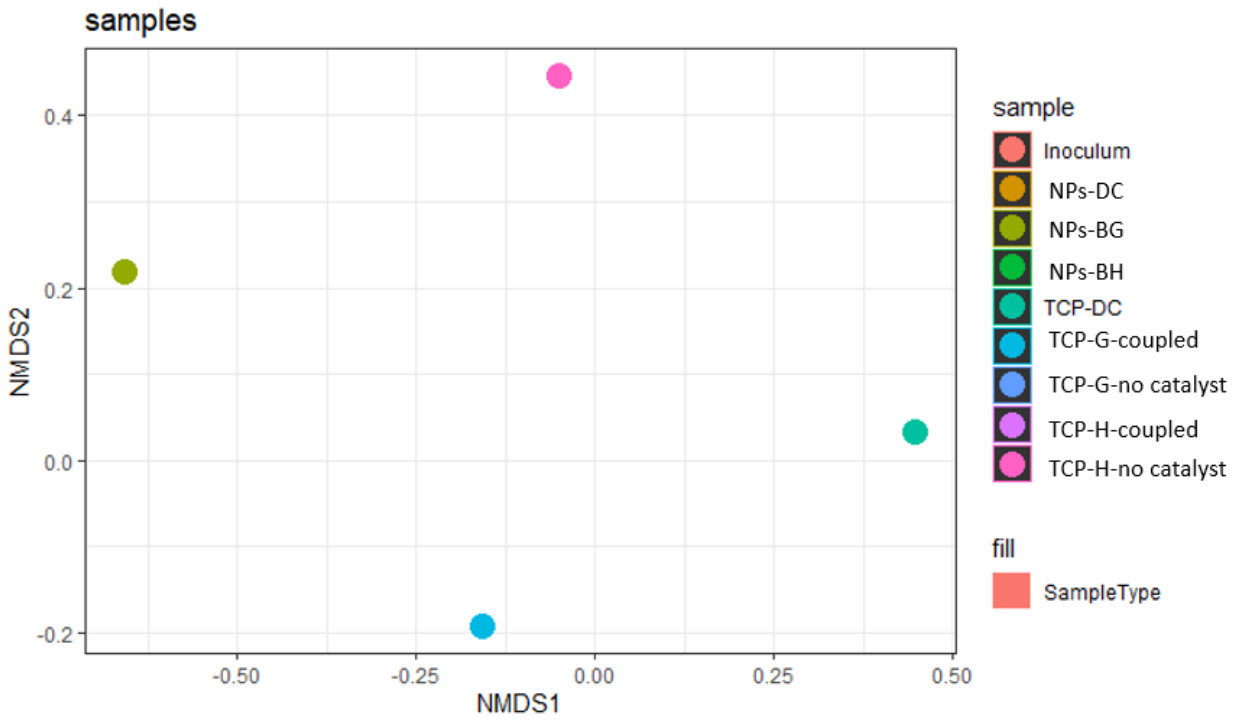

Figure 9. Betha diversity indexes for all microcosms. Where NPs-BH=NPs-Biotic H_2, NPs-BG= NPs-Biotic Glucose, and NPs-DC= NPs-Donor control; coupled= microbial consortia + Pd catalyst., no catalyst= lack of Pd catalyst, abiotic= lack of microbial consortia and TCP-DC= TCP without electron donor.

8. CONCLUSIONS AND PERSPECTIVES

This study aimed to investigate the reduction of Pd(II) through the addition of H_2 or glucose as electron donors to a synthetic medium in the presence or absence of microbial consortia. The resulting microcosms were analyzed to determine the most effective method for reducing Pd(II) and produce Pd NPs. The potential impact of different electron donors and catalysts on the resulting bacterial community structure was also addressed.

For the reduction of Pd(II), the microcosm inoculated with glucose exhibited the most pronounced efficacy in metal reduction after a 24-hour incubation period. This can be attributed to the availability of energy in specific reactions involving glucose, such as fermentation. Irrespective of inoculation status, microcosms supplemented with H_2 as the electron donor demonstrated the capacity to reduce over 95% of the Pd within the designated time frame.

Regarding the reduction of TCP, the presence of the Pd catalyst did not induce a more rapid reduction of the contaminant in systems supplemented with glucose. Under lack of Pd NPs as catalyst, the bacterial community most likely utilized TCP likely as a carbon source for cell growth and produced H_2 through glucose fermentation due to the presence of fermenters such as those from the phyla Firmicutes. Nevertheless, the Pd catalyst did promote the reduction in microcosms supplemented with hydrogen as the electron donor.

Furthermore, phylogenetic sequencing data analysis revealed that the microcosms exhibited different community structures. To some degree, the type of electron donor and the presence or absence of Pd catalyst had different impacts on the microbial communities. The *Clostridium* genus was more prominent in the inoculated microcosm with Pd(II) and glucose, but decreased with the presence of TCP. *Klebsiella* showed higher relative abundance in the inoculated microcosms with TCP. However, The genera *Azospira*, *Thauera*, and Zooglea were present in all microcosms.

Although the microcosms demonstrated a capacity for TCP reduction regardless of the type of electron donor, further investigation employing high-performance liquid chromatography-mass spectrometry (HPLC-MS) is warranted to elucidate the precise biotransformation pathway and identify the resulting transformation products

Overall, these findings highlight the feasibility of utilizing bacterial communities for the reduction of Pd(II) to be further used as catalyst. This work also builds on the state of the art for TCP microbial degradation and emphasize the relevance of

inorganic and organic electron donors when using microbial consortia capable to degrade an emerging contaminant: TCP.

Further studies to address the different properties of biologically produced NPs when using organic vs inorganic electron donor are guaranteed. Besides, the utilization of soil sediments and water contaminated with TCP, CP, or a mixture of both can be used in future studies with Pd(0) NPs as catalyst. Furthermore, it is important to note that the conducted experiments were conducted in batch reactors. Therefore, it is imperative to employ a continuous process in order to gain a more comprehensive understanding of the crucial aspects related to TCP degradation in a continouos system. This includes the synthesis of finely dispersed nano-scale particles possessing a significant surface area to facilitate enhanced catalytic reactivity, the ability to sustain such reactivity over prolonged periods of continuous operation, the continuous palladium recovery, and the assessment of the feasibility of implementing this technology at a full-scale level as a viable and efficient option.

9. REFERENCES

1. Basic Information about Pesticide Ingredients | US EPA. https://www.epa.gov/ingredients-used-pesticide-products/basic-information-about-pesticide-ingredients.
2. Yang, C., Liu, N., Guo, X., letters, C. Q.-F. microbiology & 2006, undefined. Cloning of mpd gene from a chlorpyrifos-degrading bacterium and use of this strain in bioremediation of contaminated soil. *academic.oup.com*.
3. Gwinn, M., Whipkey, D., … L. T.-E. H. & 2005, undefined. Differential gene expression in normal human mammary epithelial cells treated with malathion monitored by DNA microarrays. *ehp.niehs.nih.gov* **113**, 1046–1051 (2005).
4. Lu, P. *et al.* Biodegradation of chlorpyrifos and 3,5,6-trichloro-2-pyridinol by Cupriavidus sp. DT-1. *Bioresour Technol* **127**, 337–342 (2013).
5. OMS. *Clasificación recomendada por la OMS de los plaguicidas por el peligro que presentan y directrices para la clasificación 2019*. vol. 1 (2019).
6. John, E. M. & Shaike, J. M. Chlorpyrifos: pollution and remediation. *Environ Chem Lett* **13**, 269–291 (2015).
7. Lu, P. *et al.* Biodegradation of chlorpyrifos and 3,5,6-trichloro-2-pyridinol by Cupriavidus sp. DT-1. *Bioresour Technol* **127**, 337–342 (2013).
8. Cáceres, T., He, W., Naidu, R. & Megharaj, M. Toxicity of chlorpyrifos and TCP alone and in combination to Daphnia carinata: The influence of microbial degradation in natural water. *Water Res* **41**, 4497–4503 (2007).
9. Gilani, R. A. *et al.* Biodegradation of chlorpyrifos by bacterial genus Pseudomonas. *J Basic Microbiol* **56**, 105–119 (2016).
10. US EPA, Grube, A., Donaldson, D., Kiely, T. & Wu, L. Pesticides industry sales and usage. *US EPA, Washington, DC* 41 (2011).
11. Cáceres, T., He, W., Naidu, R. & Megharaj, M. Toxicity of chlorpyrifos and TCP alone and in combination to Daphnia carinata: The influence of microbial degradation in natural water. *Water Res* **41**, 4497–4503 (2007).
12. Mcconnell, L. L. *et al.* Chlorpyrifos in the air and surface water of Chesapeake Bay: Predictions of atmospheric deposition fluxes. *Environ Sci Technol* **31**, 1390–1398 (1997).
13. El-Kabbany, S., Rashed, M. M. & Zayed, M. A. Monitoring of the pesticide levels in some water supplies and agricultural land, in El-Haram, Giza (A.R.E.). *J Hazard Mater* **72**, 11–21 (2000).

14. Banks, K. E., Hunter, D. H. & Wachal, D. J. Chlorpyrifos in surface waters before and after a federally mandated ban. *Environ Int* **31**, 351–356 (2005).

15. Bose, S., Kumar, P. S. & Vo, D. V. N. A review on the microbial degradation of chlorpyrifos and its metabolite TCP. *Chemosphere* **283**, 131447 (2021).

16. Eaton, D. L. *et al.* Review of the toxicology of chlorpyrifos with an emphasis on human exposure and neurodevelopment. *Crit Rev Toxicol* **38**, 1–125 (2008).

17. Saini, R. & Kumar, P. Simultaneous removal of methyl parathion and chlorpyrifos pesticides from model wastewater using coagulation/flocculation: Central composite design. *J Environ Chem Eng* **4**, 673–680 (2016).

18. Suvarchala, G. & Philip, G. H. Toxicity of 3,5,6-trichloro-2-pyridinol tested at multiple stages of zebrafish (Danio rerio) development. *Environmental Science and Pollution Research* **23**, 15515–15523 (2016).

19. Bose, S., Kumar, P. S. & Vo, D. V. N. A review on the microbial degradation of chlorpyrifos and its metabolite TCP. *Chemosphere* vol. 283 Preprint at https://doi.org/10.1016/j.chemosphere.2021.131447 (2021).

20. Eaton, D. L. *et al.* Review of the toxicology of chlorpyrifos with an emphasis on human exposure and neurodevelopment. *Critical Reviews in Toxicology* vol. 38 1–125 Preprint at https://doi.org/10.1080/10408440802272158 (2008).

21. John, E. M. & Shaike, J. M. Chlorpyrifos: pollution and remediation. *Environmental Chemistry Letters* vol. 13 269–291 Preprint at https://doi.org/10.1007/s10311-015-0513-7 (2015).

22. Zhang, F. *et al.* Chlorpyrifos and 3, 5, 6-trichloro-2-pyridinol degradation in zero valent iron coupled anaerobic system: performances and mechanisms. *Elsevier*.

23. Tiwari, M. K. & Guha, S. Kinetics of biotransformation of chlorpyrifos in aqueous and soil slurry environments. *Water Res* **51**, 73–85 (2014).

24. Ambreen, S. & Yasmin, A. Novel degradation pathways for Chlorpyrifos and 3, 5, 6-Trichloro-2-pyridinol degradation by bacterial strain Bacillus thuringiensis MB497 isolated from agricultural fields of Mianwali, Pakistan. *Pestic Biochem Physiol* **172**, (2021).

25. Barr, D. B. *et al.* Concentrations of selective metabolites of organophosphorus pesticides in the United States population. *Environ Res* **99**, 314–326 (2005).

26. Watts, M. Chlorpyrifos as a possible global POP. *Pesticide Action Network North America* 1–34 (2012).

27. Saini, R. & Kumar, P. Simultaneous removal of methyl parathion and chlorpyrifos pesticides from model wastewater using coagulation/flocculation: Central composite design. *J Environ Chem Eng* **4**, 673–680 (2016).

28. Femia, J., Mariani, M., Zalazar, C. & Tiscornia, I. Photodegradation of chlorpyrifos in water by UV/H2O2 treatment: Toxicity evaluation. *Water Science and Technology* **68**, 2279–2286 (2013).

29. Hossain, M. S., Fakhruddin, A. N. M., Chowdhury, M. A. Z. & Alam, M. K. Degradation of chlorpyrifos, an organophosphorus insecticide in aqueous solution with gamma irradiation and natural sunlight. *J Environ Chem Eng* **1**, 270–274 (2013).

30. Badawy, M. I., Ghaly, M. Y. & Gad-Allah, T. A. Advanced oxidation processes for the removal of organophosphorus pesticides from wastewater. *Desalination* **194**, 166–175 (2006).

31. Bavcon Kralj, M., Franko, M. & Trebše, P. Photodegradation of organophosphorus insecticides – Investigations of products and their toxicity using gas chromatography–mass spectrometry and AChE-thermal lens spectrometric bioassay. *Chemosphere* **67**, 99–107 (2007).

32. Thind, P. S., Kumari, D. & John, S. TiO2/H2O2 mediated UV photocatalysis of Chlorpyrifos: Optimization of process parameters using response surface methodology. *J Environ Chem Eng* **6**, 3602–3609 (2018).

33. Žabar, R., Sarakha, M., Lebedev, A. T., Polyakova, O. V. & Trebše, P. Photochemical fate and photocatalysis of 3,5,6-trichloro-2-pyridinol, degradation product of chlorpyrifos. *Chemosphere* **144**, 615–620 (2016).

34. Žabar, R., Sarakha, M., Lebedev, A. T., Polyakova, O. v. & Trebše, P. Photochemical fate and photocatalysis of 3,5,6-trichloro-2-pyridinol, degradation product of chlorpyrifos. *Chemosphere* **144**, 615–620 (2016).

35. Bavcon Kralj, M., Franko, M. & Trebše, P. Photodegradation of organophosphorus insecticides - Investigations of products and their toxicity using gas chromatography-mass spectrometry and AChE-thermal lens spectrometric bioassay. *Chemosphere* **67**, 99–107 (2007).

36. Zamy, C., Mazellier, P. & Legube, B. Phototransformation of selected organophosphorus pesticides in dilute aqueous solutions. *Water Res* **38**, 2305–2314 (2004).

37. John, E. M. & Shaike, J. M. Chlorpyrifos: pollution and remediation. *Environmental Chemistry Letters* vol. 13 269–291 Preprint at https://doi.org/10.1007/s10311-015-0513-7 (2015).

38. Bondarenko, S., Gan, J., Haver, D. L. & Kabashima, J. N. Persistence of selected organophosphate and carbamate insecticides in waters from a coastal watershed. *Environ Toxicol Chem* **23**, 2649–2654 (2004).

39. Krishna, K. R. & Philip, L. Biodegradation of lindane, methyl parathion and carbofuran by various enriched bacterial isolates. *J Environ Sci Health B* **43**, 157–171 (2008).

40. John, E. M., Sreekumar, J. & Jisha, M. S. Optimization of Chlorpyrifos Degradation by Assembled Bacterial Consortium Using Response Surface Methodology. *Soil Sediment Contam* **25**, 668–682 (2016).

41. Mali, H. *et al.* Organophosphate pesticides an emerging environmental contaminant: Pollution, toxicity, bioremediation progress, and remaining challenges. *Journal of Environmental Sciences (China)* vol. 127 234–250 Preprint at https://doi.org/10.1016/j.jes.2022.04.023 (2023).

42. Sidhu, G. K. *et al.* Toxicity, monitoring and biodegradation of organophosphate pesticides: A review. *Crit Rev Environ Sci Technol* **49**, 1135–1187 (2019).

43. Yang, L., Zhao, Y. H., Zhang, B. X., Yang, C. H. & Zhang, X. Isolation and characterization of a chlorpyrifos and 3,5,6-trichloro-2- pyridinol degrading bacterium. *FEMS Microbiol Lett* **251**, 67–73 (2005).

44. Yang, L., Zhao, Y. H., Zhang, B. X., Yang, C. H. & Zhang, X. Isolation and characterization of a chlorpyrifos and 3,5,6-trichloro-2- pyridinol degrading bacterium. *FEMS Microbiol Lett* **251**, 67–73 (2005).

45. Singh, B. K., Walker, A., Morgan, J. A. W. & Wright, D. J. Biodegradation of chlorpyrifos by Enterobacter strain B-14 and its use in bioremediation of contaminated soils. *Appl Environ Microbiol* **70**, 4855–4863 (2004).

46. Li, J. *et al.* Isolation and characterization of 3,5,6-trichloro-2-pyridinol-degrading Ralstonia sp. strain T6. *Bioresour Technol* **101**, 7479–7483 (2010).

47. Anwar, S., Liaquat, F., Khan, Q. M., Khalid, Z. M. & Iqbal, S. Biodegradation of chlorpyrifos and its hydrolysis product 3,5,6-trichloro-2-pyridinol by Bacillus pumilus strain C2A1. *J Hazard Mater* **168**, 400–405 (2009).

48. Kulshrestha, G. & Kumari, A. Fungal degradation of chlorpyrifos by Acremonium sp. strain (GFRC-1) isolated from a laboratory-enriched red agricultural soil. *Biol Fertil Soils* **47**, 219–225 (2011).

49. Kim, J. R. & Ahn, Y. J. Identification and characterization of chlorpyrifos-methyl and 3,5,6-trichloro-2-pyridinol degrading Burkholderia sp. strain KR100. *Biodegradation* **20**, 487–497 (2009).

50. Xu, G. *et al.* Biodegradation of chlorpyrifos and 3,5,6-trichloro-2-pyridinol by a newly isolated Paracoccus sp. strain TRP. *Int Biodeterior Biodegradation* **62**, 51–56 (2008).

51. Mali, H., Shah, C., Patel, D. H., Trivedi, U. & Subramanian, R. B. Degradation insight of organophosphate pesticide chlorpyrifos through novel intermediate 2,6-dihydroxypyridine by Arthrobacter sp. HM01. *Bioresour Bioprocess* **9**, (2022).

52. Ambreen, S. & Yasmin, A. Novel degradation pathways for Chlorpyrifos and 3, 5, 6-Trichloro-2-pyridinol degradation by bacterial strain Bacillus thuringiensis MB497 isolated from agricultural fields of Mianwali, Pakistan. *Pestic Biochem Physiol* **172**, (2021).

53. Abraham, J. & Silambarasan, S. Biodegradation of chlorpyrifos and its hydrolyzing metabolite 3,5,6-trichloro-2-pyridinol by Sphingobacterium sp. JAS3. *Process Biochemistry* **48**, 1559–1564 (2013).

54. Verma, S., Singh, D. & Chatterjee, S. Biodegradation of organophosphorus pesticide chlorpyrifos by Sphingobacterium sp. C1B, a psychrotolerant bacterium isolated from apple orchard in Himachal Pradesh of India. *Extremophiles* **24**, 897–908 (2020).

55. Kuppusamy, S., Thavamani, P., … M. M.-I. & 2016, undefined. Biodegradation of polycyclic aromatic hydrocarbons (PAHs) by novel bacterial consortia tolerant to diverse physical settings–assessments in liquid-and slurry. *Elsevier*.

56. Pino, N. & Peñuela, G. Simultaneous degradation of the pesticides methyl parathion and chlorpyrifos by an isolated bacterial consortium from a contaminated site. *Int Biodeterior Biodegradation* **65**, 827–831 (2011).

57. John, E. M., Sreekumar, J. & Jisha, M. S. Optimization of Chlorpyrifos Degradation by Assembled Bacterial Consortium Using Response Surface Methodology. *Soil Sediment Contam* **25**, 668–682 (2016).

58. Abraham, J. & Silambarasan, S. Biodegradation of chlorpyrifos and 3,5,6-trichloro-2-pyridinol by fungal consortium isolated from paddy field soil. *Environ Eng Manag J* **17**, 523–528 (2018).

59. Wang, S. *et al.* Degradation of 3,5,6-trichloro-2-pyridinol by a microbial consortium in dryland soil with anaerobic incubation. *Biodegradation* (2019) doi:10.1007/S10532-019-09873-Y.

60. Sun, X. *et al.* Biodegradation of CP/TCP by a constructed microbial consortium after comparative bacterial community analysis of long-term CP domesticated activated sludge. *J Environ Sci Health B* 898–908 (2020) doi:10.1080/03601234.2020.1794453.

61. Uniyal, S., Sharma, R. K. & Kondakal, V. New insights into the biodegradation of chlorpyrifos by a novel bacterial consortium: Process optimization using general factorial experimental design. *Ecotoxicol Environ Saf* **209**, (2021).

62. Gauthard, F., Epron, F., Catalysis, J. B.-J. of & 2003, undefined. Palladium and platinum-based catalysts in the catalytic reduction of nitrate in water: effect of copper, silver, or gold addition. *Elsevier*.

63. Hydrometallurgy, N. D.- & 2010, undefined. Recovery of precious metals through biosorption—a review. *Elsevier*.

64. Chaplin, B. P. *et al.* Critical review of Pd-based catalytic treatment of priority contaminants in water. *Environmental Science and Technology* vol. 46 3655–3670 Preprint at https://doi.org/10.1021/es204087q (2012).

65. Sau, T., Materials, A. R.-A. & 2010, undefined. Nonspherical noble metal nanoparticles: colloid-chemical synthesis and morphology control. *Wiley Online Library* **22**, 1781–1804 (2010).

66. Sci-Hub | Synthesis and Characterization of Gold Nanoparticles by Tryptophane. American Journal of Applied Sciences, 6(4), 691–695 | 10.3844/ajassp.2009.691.695. https://sci-hub.se/10.3844/ajassp.2009.691.695.

67. Pat-Espadas, A. M. *et al.* Recovery of palladium(II) by methanogenic granular sludge. *Chemosphere* **144**, 745–753 (2016).

68. De Corte, S., Hennebel, T., De Gusseme, B., Verstraete, W. & Boon, N. Bio-palladium: From metal recovery to catalytic applications. *Microb Biotechnol* **5**, 5–17 (2012).

69. Hulkoti, N. I. & Taranath, T. C. Biosynthesis of nanoparticles using microbes—A review. *Colloids Surf B Biointerfaces* **121**, 474–483 (2014).

70. Zhang, X., Yan, S., Tyagi, R. D. & Surampalli, R. Y. Synthesis of nanoparticles by microorganisms and their application in enhancing microbiological reaction rates. *Chemosphere* **82**, 489–494 (2011).

71. Pat-Espadas, A. M. *et al.* Immobilization of biogenic Pd(0) in anaerobic granular sludge for the biotransformation of recalcitrant halogenated pollutants in UASB reactors. *Appl Microbiol Biotechnol* **100**, 1427–1436 (2016).

72. Rashamuse, K. J. & Whiteley, C. G. Bioreduction of Pt (IV) from aqueous solution using sulphate-reducing bacteria. *Appl Microbiol Biotechnol* **75**, 1429–1435 (2007).

73. Lloyd, J. R., Yong, P. & Macaskie, L. E. Enzymatic recovery of elemental palladium by using sulfate-reducing bacteria. *Appl Environ Microbiol* **64**, 4607–4609 (1998).

74. Windt, W. de, Aelterman, P. & Verstraete, W. Bioreductive deposition of palladium (0) nanoparticles on Shewanella oneidensis with catalytic activity towards reductive dechlorination of polychlorinated biphenyls. *Environ Microbiol* **7**, 314–325 (2005).

75. Yates, M. D., Cusick, R. D. & Logan, B. E. Extracellular palladium nanoparticle production using geobacter sulfurreducens. *ACS Sustain Chem Eng* **1**, 1165–1171 (2013).

76. Pat-Espadas, A. M., Razo-Flores, E., Rangel-Mendez, J. R. & Cervantes, F. J. Reduction of palladium and production of nano-catalyst by Geobacter sulfurreducens. *Appl Microbiol Biotechnol* **97**, 9553–9560 (2013).

77. Pat-Espadas, A. M., Razo-Flores, E., Rangel-Mendez, J. R. & Cervantes, F. J. Direct and quinone-mediated palladium reduction by Geobacter sulfurreducens: Mechanisms and modeling. *Environ Sci Technol* **48**, 2910–2919 (2014).

78. Konishi, Y., Ohno, K., Saitoh, N., … T. N.-J. of & 2007, undefined. Bioreductive deposition of platinum nanoparticles on the bacterium Shewanella algae. *Elsevier*.

79. Capeness, M. J., Edmundson, M. C. & Horsfall, L. E. Nickel and platinum group metal nanoparticle production by Desulfovibrio alaskensis G20. *N Biotechnol* **32**, 727–731 (2015).

80. Ahmad, A. *et al.* Intracellular synthesis of gold nanoparticles by a novel alkalotolerant actinomycete, Rhodococcus species. *iopscience.iop.org* **14**, 824–828 (2003).

81. Parikh, R. Y. *et al.* Extracellular synthesis of crystalline silver nanoparticles and molecular evidence of silver resistance from Morganella sp.: Towards understanding biochemical synthesis mechanism. *ChemBioChem* **9**, 1415–1422 (2008).

82. Shahverdi, A., Fakhimi, A., … H. S.-, Medicine, B. and & 2007, undefined. Synthesis and effect of silver nanoparticles on the antibacterial activity of different antibiotics against Staphylococcus aureus and Escherichia coli. *Elsevier*.

83. Sinha, A., Technology, S. K.-B. & 2011, undefined. Mercury bioaccumulation and simultaneous nanoparticle synthesis by Enterobacter sp. cells. *Elsevier*.

84. Chaplin, B. P. *et al.* Critical review of Pd-based catalytic treatment of priority contaminants in water. *Environ Sci Technol* **46**, 3655–3670 (2012).

85. Figueras, F., Chemical, B. C.-J. of M. C. A. & 2001, undefined. Hydrogenation and hydrogenolysis of nitro-, nitroso-, azo-, azoxy-and other nitrogen-containing compounds on palladium. *Elsevier*.

86. Urbano, F., Chemical, J. M.-J. of M. C. A. & 2001, undefined. Hydrogenolysis of organohalogen compounds over palladium supported catalysts. *Elsevier*.

87. Danmeng, S. *et al.* Enhancement of oxyanion and diatrizoate reduction kinetics using selected azo dyes on Pd-based catalysts. *Environ Sci Technol* **44**, 1773–1779 (2010).

88. Lowry, G., Technology, M. R.-E. S. & & 1999, undefined. Hydrodehalogenation of 1-to 3-carbon halogenated organic compounds in water using a palladium catalyst and hydrogen gas. *ACS Publications* **33**, 1905–1910 (1999).

89. Schreier, C., Chemosphere, M. R.- & 1995, undefined. Catalytic hydrodehalogenation of chlorinated ethylenes using palladium and hydrogen for the treatment of contaminated water. *Elsevier*.

90. Zhou, C. *et al.* Coupling of Pd nanoparticles and denitrifying biofilm promotes H2-based nitrate removal with greater selectivity towards N2. *Appl Catal B* **206**, 461–470 (2017).

91. Greenwood, N. N. & Earnshaw, A. Chemistry of the Elements. (2012).

92. Pat-Espadas, A. M., Razo-Flores, E., Rangel-Mendez, J. R. & Cervantes, F. J. Direct and quinone-mediated palladium reduction by Geobacter sulfurreducens: Mechanisms and modeling. *Environ Sci Technol* **48**, 2910–2919 (2014).

93. De Corte, S., Hennebel, T., De Gusseme, B., Verstraete, W. & Boon, N. Bio-palladium: From metal recovery to catalytic applications. *Microb Biotechnol* **5**, 5–17 (2012).

94. Windt, W. De, Aelterman, P. & Verstraete, W. Bioreductive deposition of palladium (0) nanoparticles on Shewanella oneidensis with catalytic activity towards reductive dechlorination of polychlorinated biphenyls. *Environ Microbiol* **7**, 314–325 (2005).

95. Lloyd, J. R., Yong, P. & Macaskie, L. E. Enzymatic recovery of elemental palladium by using sulfate-reducing bacteria. *Appl Environ Microbiol* **64**, 4607–4609 (1998).

96. Pat-Espadas, A. M., Razo-Flores, E., Rangel-Mendez, J. R. & Cervantes, F. J. Reduction of palladium and production of nano-catalyst by Geobacter sulfurreducens. *Appl Microbiol Biotechnol* **97**, 9553–9560 (2013).

97. Pat-Espadas, A. M. *et al.* Recovery of palladium(II) by methanogenic granular sludge. *Chemosphere* **144**, 745–753 (2016).

98. Martins, M., Assunção, A., Martins, H., Matos, A. P. & Costa, M. C. Palladium recovery as nanoparticles by an anaerobic bacterial community. *Journal of Chemical Technology and Biotechnology* **88**, 2039–2045 (2013).

99. Zhou, C. *et al.* Palladium Recovery in a H2-Based Membrane Biofilm Reactor: Formation of Pd(0) Nanoparticles through Enzymatic and Autocatalytic Reductions. *Environ Sci Technol* **50**, 2546–2555 (2016).

100. Pat-Espadas, A. M. *et al.* Immobilization of biogenic Pd(0) in anaerobic granular sludge for the biotransformation of recalcitrant halogenated pollutants in UASB reactors. *Appl Microbiol Biotechnol* **100**, 1427–1436 (2016).

101. Long, M. *et al.* Para-Chlorophenol (4-CP) Removal by a Palladium-Coated Biofilm: Coupling Catalytic Dechlorination and Microbial Mineralization via Denitrification. *Environ Sci Technol* **55**, 6309–6319 (2021).

102. Forrez, I. *et al.* Biogenic metals for the oxidative and reductive removal of pharmaceuticals, biocides and iodinated contrast media in a polishing membrane bioreactor. *Water Res* **45**, 1763–1773 (2011).

103. Hennebel, T., de Gusseme, B., Boon, N. & Verstraete, W. Biogenic metals in advanced water treatment. *Trends in Biotechnology* vol. 27 90–98 Preprint at https://doi.org/10.1016/j.tibtech.2008.11.002 (2009).

104. Zhou, C. *et al.* Coupling of Pd nanoparticles and denitrifying biofilm promotes H2-based nitrate removal with greater selectivity towards N2. *Appl Catal B* **206**, 461–470 (2017).

105. Zhou, C. *et al.* Palladium Recovery in a H2-Based Membrane Biofilm Reactor: Formation of Pd(0) Nanoparticles through Enzymatic and Autocatalytic Reductions. *Environ Sci Technol* **50**, 2546–2555 (2016).

106. Long, M. *et al.* Para-Chlorophenol (4-CP) Removal by a Palladium-Coated Biofilm: Coupling Catalytic Dechlorination and Microbial Mineralization via Denitrification. *Environ Sci Technol* **55**, 6309–6319 (2021).

107. Ontiveros-Valencia, A., Penton, C. R., Krajmalnik-Brown, R. & Rittmann, B. E. Hydrogen-fed biofilm reactors reducing selenate and sulfate: Community structure and capture of elemental selenium within the biofilm. *Biotechnol Bioeng* **113**, 1736–1744 (2016).

108. Pat-Espadas, A. M. *et al.* Recovery of palladium(II) by methanogenic granular sludge. *Chemosphere* **144**, 745–753 (2016).

109. Caporaso, J. G. *et al.* Global patterns of 16S rRNA diversity at a depth of millions of sequences per sample. *Proc Natl Acad Sci U S A* **108**, 4516–4522 (2011).

110. Callahan, B. J. *et al.* DADA2: High-resolution sample inference from Illumina amplicon data. *Nat Methods* **13**, 581–583 (2016).

111. McLaren, M. R. & Callahan, B. J. Silva 138.1 prokaryotic SSU taxonomic training data formatted for DADA2. (2021) doi:10.5281/ZENODO.4587955.

112. McMurdie, P. J. & Holmes, S. Phyloseq: An R Package for Reproducible Interactive Analysis and Graphics of Microbiome Census Data. *PLoS One* **8**, (2013).

113. Zhou, C. *et al.* Palladium Recovery in a H2-Based Membrane Biofilm Reactor: Formation of Pd(0) Nanoparticles through Enzymatic and Autocatalytic Reductions. *Environ Sci Technol* **50**, 2546–2555 (2016).

114. Zhou, C. *et al.* Coupling of Pd nanoparticles and denitrifying biofilm promotes H2-based nitrate removal with greater selectivity towards N2. *Appl Catal B* **206**, 461–470 (2017).

115. Martins, M., Assunção, A., Martins, H., Matos, A. P. & Costa, M. C. Palladium recovery as nanoparticles by an anaerobic bacterial community. *Journal of Chemical Technology and Biotechnology* **88**, 2039–2045 (2013).

116. Rotaru, A.-E., Jiang, W., Finster, K., Skrydstrup, T. & Meyer, R. L. EDITORS' CHOICE Non-Enzymatic Palladium Recovery on Microbial and Synthetic Surfaces. *Biotechnol. Bioeng* **109**, 1889–1897 (2012).

117. Hennebel, T. *et al.* Palladium nanoparticles produced by fermentatively cultivated bacteria as catalyst for diatrizoate removal with biogenic hydrogen. *Appl Microbiol Biotechnol* **91**, 1435–1445 (2011).

118. Hou, T., Zhang, S., Chen, Y., Wang, D. & Cai, W. Hydrogen production from ethanol reforming: Catalysts and reaction mechanism. *Renewable and Sustainable Energy Reviews* vol. 44 132–148 Preprint at https://doi.org/10.1016/j.rser.2014.12.023 (2015).

119. Hou, T., Zhang, S., Chen, Y., Wang, D. & Cai, W. Hydrogen production from ethanol reforming: Catalysts and reaction mechanism. *Renewable and Sustainable Energy Reviews* vol. 44 132–148 Preprint at https://doi.org/10.1016/j.rser.2014.12.023 (2015).

120. Rotaru, A.-E., Jiang, W., Finster, K., Skrydstrup, T. & Meyer, R. L. EDITORS' CHOICE Non-Enzymatic Palladium Recovery on Microbial and Synthetic Surfaces. *Biotechnol. Bioeng* **109**, 1889–1897 (2012).

121. Zhang, F. *et al.* Chlorpyrifos and 3,5,6-trichloro-2-pyridinol degradation in zero valent iron coupled anaerobic system: Performances and mechanisms. *Chemical Engineering Journal* **353**, 254–263 (2018).

122. Zhou, C. *et al.* Coupling of Pd nanoparticles and denitrifying biofilm promotes H2-based nitrate removal with greater selectivity towards N2. *Appl Catal B* **206**, 461–470 (2017).

123. Zhou, C. *et al.* Uranium removal and microbial community in a H2-based membrane biofilm reactor. *Water Res* **64**, 255–264 (2014).

124. Pat-Espadas, A. M. *et al.* Immobilization of biogenic Pd(0) in anaerobic granular sludge for the biotransformation of recalcitrant halogenated pollutants in UASB reactors. *Appl Microbiol Biotechnol* **100**, 1427–1436 (2016).

125. Long, M. *et al.* Para-Chlorophenol (4-CP) Removal by a Palladium-Coated Biofilm: Coupling Catalytic Dechlorination and Microbial Mineralization via Denitrification. *Environ Sci Technol* **55**, 6309–6319 (2021).

126. Cai, Y., Long, X., Luo, Y. H., Zhou, C. & Rittmann, B. E. Stable dechlorination of Trichloroacetic Acid (TCAA) to acetic acid catalyzed by palladium nanoparticles deposited on H2-transfer membranes. *Water Res* **192**, 116841 (2021).

127. Simon de Corte_Biopalladium_from metal recovery to catalytic applications.

128. Maya, K., Singh, R. S., Upadhyay, S. N. & Dubey, S. K. Kinetic analysis reveals bacterial efficacy for biodegradation of chlorpyrifos and its hydrolyzing metabolite TCP. *Process Biochemistry* **46**, 2130–2136 (2011).

129. Feng, L. J., Yang, G. F., Zhu, L. & Xu, X. Y. Removal performance of nitrogen and endocrine-disrupting pesticides simultaneously in the enhanced biofilm system for polluted source water pretreatment. *Bioresour Technol* **170**, 549–555 (2014).

130. Yang, G., Yin, Y. & Wang, J. Microbial community diversity during fermentative hydrogen production inoculating various pretreated cultures. *Int J Hydrogen Energy* **44**, 13147–13156 (2019).

131. Zhang, F. *et al.* Chlorpyrifos and 3,5,6-trichloro-2-pyridinol degradation in zero valent iron coupled anaerobic system: Performances and mechanisms. *Chemical Engineering Journal* **353**, 254–263 (2018).

132. Ginige, M. P., Keller, J. & Blackall, L. L. Investigation of an acetate-fed denitrifying microbial community by stable isotope probing, full-cycle rRNA analysis, and fluorescent in situ hybridization-microautoradiography. *Appl Environ Microbiol* **71**, 8683–8691 (2005).

133. Chidambaram, D., Hennebel, T., technology, S. T.-… science & & 2010, undefined. Concomitant microbial generation of palladium nanoparticles and hydrogen to immobilize chromate. *ACS Publications* **44**, 7635–7640 (2010).

134. Francis, A. J. & Dodge, C. J. Effects of lead oxide and iron on glucose fermentation by Clostridium sp. *Arch Environ Contam Toxicol* **16**, 491–497 (1987).

135. Rosenberg, E., Delong, E.-I.-C. E. F., Lory, S., Stackebrandt, E. & Thompson, F. *The Prokaryotes*.

136. Rolighed Thomsen, T., Kong, Y. & Halkjaer Nielsen, P. Ecophysiology of abundant denitrifying bacteria in activated sludge. doi:10.1111/j.1574-6941.2007.00309.x.

137. Slezak, R., Grzelak, J., Krzystek, L., Management, S. L.-W. & 2017, undefined. The effect of initial organic load of the kitchen waste on the production of VFA and H2 in dark fermentation. *Elsevier*.

138. Yang, S. T. Bioprocessing for value-added products from renewable resources: New technologies and applications. *Bioprocessing for Value-Added Products from Renewable Resources: New Technologies and Applications* 1–670 (2006) doi:10.1016/B978-0-444-52114-9.X5000-2.